Regional heterogeneities in the emission of airborne primary sugar compounds and biogenic secondary organic aerosols in the East Asian outflow: Evidence for coal combustion as a source of levoglucosan

M. Mozammel Haque[1,2,3], Yanlin Zhang[1,2*] Srinivas Bikkina[4], Meehye Lee[5], and Kimitaka Kawamura[3,4*]

[1]*Yale-NUIST Center on Atmospheric Environment, International Joint Laboratory on Climate and Environment Change (ILCEC), Nanjing University of Information Science & Technology, Nanjing, 210044, China*
[2]*School of Applied Meteorology, Nanjing University of Information Science & Technology, Nanjing 210044, China*
[3]*Institute of Low Temperature Science, Hokkaido University, Sapporo 060-0819, Japan*
[4]*Chubu Institute for Advanced Studies, Chubu University, Kasugai 487-8501, Japan*
[5]*Department of Earth and Environmental Sciences, Korea University, Anam-dong, Sungbuk-gu, Seoul 136-701, South Korea*

Corresponding author
E-mail: dryanlinzhang@outlook.com (Yan-Lin Zhang)
E-mail: kkawamura@isc.chubu.ac.jp (Kimitaka Kawamura)

ABSTRACT

Biomass burning (BB) significantly influences the chemical composition of organic aerosols (OA) in the East Asian outflow. Source apportionment of BB-derived OA is an influential factor for understanding their regional emissions, which is crucial for reducing uncertainties in their projected climate and health-effects. We analyzed here three different classes of atmospheric sugar compounds (anhydrosugars, primary sugars, and sugar alcohols) and two types of biogenic secondary organic aerosol (BSOA) tracers (isoprene- and monoterpene derived SOA products) in a year-long collected total suspended particulate matter (TSP) from an island-based receptor site in South Korea, Gosan. We investigate seasonal variations in the source-emissions of BB-derived OA using mass concentrations of anhydrosugars and radiocarbon (^{14}C-) isotopic composition of organic carbon (OC) and elemental carbon (EC) in ambient aerosols. Levoglucosan (*Lev*) is the most abundant anhydrosugar, followed by galactosan (*Gal*) and mannosan (*Man*). Strong correlations of *Lev* with *Gal* and *Man*, along with their ratios (*Lev*/*Gal:* 6.65 ± 2.26; *Lev*/*Man*: 15.1 ± 6.76) indicate the contribution from hardwood burning emissions. The seasonal trends revealed that the BB impact is more pronounced in winter and fall, as evidenced by the high concentrations of anhydrosugars. Likewise, significant correlations among three primary sugars (i.e., glucose, fructose, and sucrose) emphasized the contribution of airborne pollen. The primary sugars showed higher concentrations in spring/summer than winter/fall. The fungal spore tracer compounds (i.e., arabitol, mannitol, and erythritol) correlated well with trehalose (i.e., a proxy for soil organic carbon), suggesting the origin from airborne fungal spores and soil microbes in the East Asian outflow. These sugar alcohols peaked in summer, followed by spring/fall and winter. Monoterpene-derived SOA tracers were most abundant compared to isoprene-SOA tracers. Both BSOA tracers were dominant in summer, followed by fall, spring, and winter. The source apportionment based on multiple linear regressions and diagnostic mass ratios together revealed that BB emission mostly contributed from hardwood and crop-residue burning. We also found significant positive linear relationships of ^{14}C-based nonfossil- and fossil-derived organic carbon fractions with *Lev-C* along with the comparable regression slopes, suggesting the importance of BB and coal combustion sources in the East Asian outflow.

Keywords: Biomass burning tracers, primary biological aerosol particles, biogenic SOA tracers, radiocarbon-based source apportionment, organic aerosols, East Asian outflow

1. Introduction

Organic aerosols (OA), which account for a major fraction of up to 50% of airborne total suspended particulate matter, have considerable effects on regional and global climate by absorbing or scattering sunlight (Kanakidou et al., 2005). However, the climate effects of OA are involved with large uncertainties due to our limited understanding of the contributing sources. OA can be derived from both primary emissions and secondarily formed species. Sugars are an important group of water-soluble, primary organic compounds whose concentrations are significant in atmospheric aerosols over the continent (Jia and Fraser, 2011; Fu et al., 2008; Yttri et al., 2007; Graham et al., 2003). Anhydrosugars such as levoglucosan, galactosan, and mannosan are the key tracers of biomass burning (BB) emissions (Simoneit, 2002). Sugar alcohols, along with glucose, trehalose and sucrose are mostly originated from primary biological particles such as fungal spores, pollen, bacteria, and viruses, and vegetative debris (Graham et al., 2003; Simoneit et al., 2004a; Bauer et al., 2008; Deguillaume et al., 2008). Primary sugars and sugar alcohols are predominantly present in the coarse mode aerosols, accounting for 0.5-10% of atmospheric aerosol carbon matter (Yttri et al., 2007; Pio et al., 2008).

Secondary organic aerosol (SOA) is a large fraction of OA, while there were only limited studies about the key factors controlling SOA formation. The SOA formation significantly increased with the enhancement of the ambient aerosol mass (Liu et al., 2018). SOA is formed by both homogenous and heterogeneous reactions of volatile organic compounds (VOCs) in the atmosphere (Surratt et al., 2010; Robinson et al., 2007; Claeys et al., 2004). On a global estimation, biogenic VOCs (BVOCs) such as isoprene, monoterpenes (e.g., α/β-pinene), and sesquiterpenes (e.g., β-caryophyllene) are one order of magnitude higher than those of anthropogenic VOCs (e.g., toluene) (Guenther et al., 2006). The global emissions of annual BVOCs were estimated to be 1150 TgC yr^{-1}, accounting for 44% isoprene and 11% monoterpenes (Guenther et al., 1995). Isoprene is highly reactive and promptly reacts with oxidants such as O_3, OH, and NO_x in the atmosphere to form SOA (Kroll et al., 2005, 2006; Ng et al., 2008; Surratt et al., 2010; Bikkina et al., 2021), estimated to be 19.2 TgC yr^{-1}, consisting of ~70% of the total SOA budget (Heald et al., 2008). Monoterpenes are important sources of biogenic secondary organic aerosol (BSOA), considering α-pinene as major species, accounting for ~35% of the global monoterpenes emissions (Griffin et al., 1999).

Anthropogenic activities such as coal and biofuel combustion over East Asia, including China, are responsible for the vast emission of OA (Huebert et al., 2003; Zhang et

al., 2016). Understanding the ambient levels OA in the East Asian outflow is crucial for assessing their regional climatic effects. As part of this effort, the Korean Climate Observatory at Gosan (KCOG), a super site located in South Korea, is an ideal location for investigating the atmospheric outflow characteristics from East Asia (Fu et al., 2010a; Kundu et al., 2010; Ramanathan et al., 2007; Kawamura et al., 2004; Arimoto et al., 1996). For instance, primary OA associated with soil/desert dust in East Asia, along with forest fires in Siberia/northeastern China, are transported over Gosan in spring (Wang et al., 2009a). BSOA during long-range transport from the continent and Open Ocean, as well as local vegetation, can significantly contribute to Gosan aerosols. Although these investigations were carried out almost a decade ago, no such observations are available in contemporary times from Gosan. Here, we attempt to understand the current states of East Asian OA using both the molecular marker approach and radiocarbon data of carbonaceous components.

The KCOG, located on the western side of Jeju Island adjacent to the Yellow Sea and the East China Sea, is facing the Asian continent but is isolated from public areas of the island (Kawamura et al., 2004). Simoneit et al. (2004b) have documented during the ACE-Asia campaign that OA from the BB and fossil fuel combustion sources are transported along with desert dust to the KCOG during continental outflow. An intensive campaign was organized at the KCOG during spring 2005 to observe the physical properties of East Asian aerosols while two dust events were detected (Nakajima et al., 2007). Here, we focus on the characterization of airborne anhydrosugars, primary sugars, sugar alcohols, and BSOA tracers from the KCOG. Gosan is influenced by the continental outflow from East Asia during winter, spring and fall, whereas the site is influenced by the maritime air masses from the Pacific Ocean and other marginal seas. This makes the KCOG ideal for characterizing the regional heterogeneities in the emissions of organic compounds in the East Asian outflow based on the TSP samples collected during April 2013-April 2014.

2. Methods

2.1. Aerosol sampling and prevailing meteorology

Total suspended particles (TSP) were collected on pre-combusted (450°C for 6 h) quartz fiber filters (20 cm × 25 cm, Pallflex) at the KCOG (33.17 °N, 126.10 °E, see Figure 1), South Korea. To get enough signal for the radiocarbon measurements, each TSP sample was collected for 10–14 days from April 2013 to April 2014. Twenty-one samples were collected using a high-volume air sampler (Kimoto AS-810, ~65 m^3 h^{-1}) installed on the rooftop of a trailer house (~3 m above the ground). After the collection, aerosol filters were transferred to a pre-combusted (450°C for 6 h) glass jar (150 mL) equipped with a Teflon-lined screw cap

and transported to the laboratory in Sapporo. These TSP samples were stored in a dark freezer room at -20°C until the analysis. Three field blank filters were also collected during the campaign.

The ambient temperatures at the Gosan site were on average 6.9°C in winter, 14.1°C in spring, 27.0°C in summer, and 17.1°C in fall. Likewise, the average relative humidity was found to be highest in summer (71.3%), followed by spring (64.9%), fall (63.5%), and winter (54.7%). Gosan is influenced by the pollution sources in East Asia during winter as well as other transition periods (spring and fall) due to the prevailing westerlies. In contrast, winds in summer blew mostly from the western North Pacific (WNP) by the easterly winds. The spring season is, in particular, important for the transport of mineral dust mixed with polluted OA to Gosan (Kundu et al., 2010).

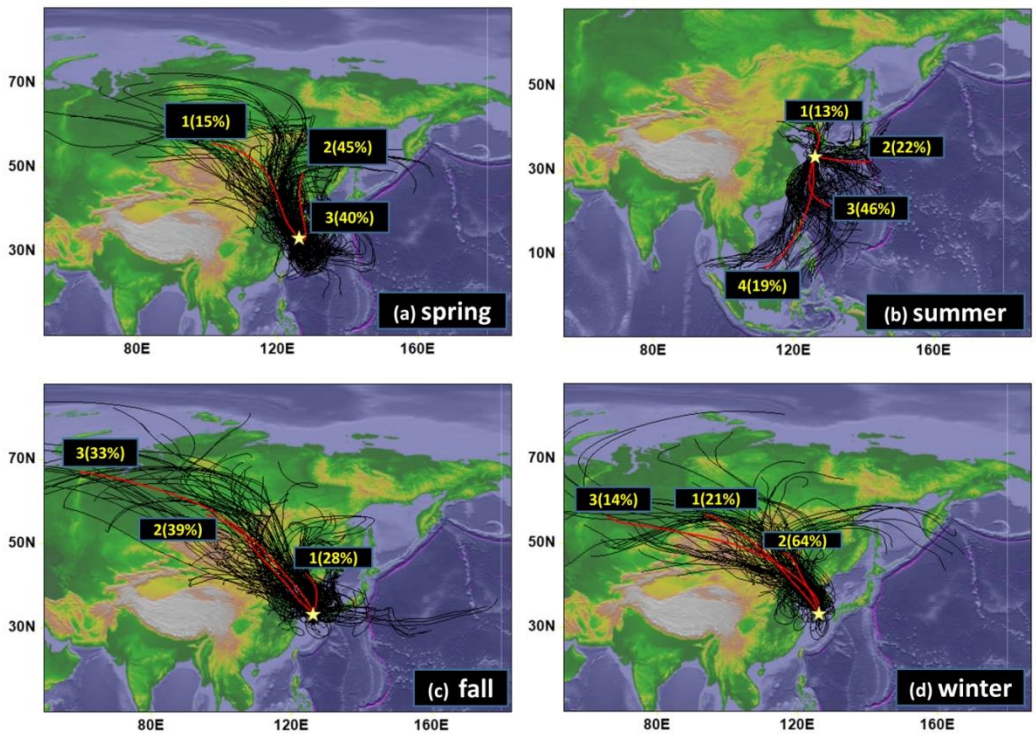

Figure 1. Cluster analysis of backward air mass trajectories over Gosan (indicated by a star symbol) for the TSP collected during (a) spring, (b) summer, (c) fall, and (d) winter seasons.

2.2. Extraction and analysis of organic compounds

Approximately 3.14 cm^2 filter cuts were extracted with dichloromethane/methanol (2:1; v/v). The extracts were concentrated using a rotary evaporator under vacuum and then blown down to near dryness with pure nitrogen gas. The dried residues were subsequently reacted with N,

O-bis(trimethylsilyl)trifluoroacetamide containing 1% trimethylchlorosilane (BSTFA+1% TMCS, SUPELCO©, Sigma-Aldrich ®) and pyridine at 70 °C for 3 h to derive OH and COOH groups of polar organic compounds to trimethylsilyl ethers and esters, respectively. After the derivatization followed by the addition of a known amount of internal standard solution (Tridecane; 1.43 ng L^{-1} in n-hexane), the derivatized extracts were injected onto a gas chromatograph (Hewlett-Packard model 6890 GC) coupled to a mass spectrometer (Hewlett-Packard model 5973, MSD) (GC-MS). More details on the quantification of polar organic compounds using GC-MS are described in Haque et al. (2019).

The target compounds (anhydrosugars, primary sugars, sugar alcohols, and BSOA tracers) were separated on a DB-5MS fused silica capillary column (30 m x 0.25 mm i.d., 0.5 μm film thickness) using helium as a carrier gas at a flow rate of 1.0 ml min^{-1}. The GC oven temperature was programmed from 50°C for 2 min and then increased from 50 to 120°C at 30°C min^{-1} and to 300°C at 6°C min^{-1} with a final isotherm hold at 300°C for 16 min. The sample was injected in a splitless mode with the injector temperature at 280°C. The MS was operated at 70 eV and scanned from 50 to 650 Da on an electron impact (EI) mode. Mass spectral data were acquired and processed using the Chemstation software. The organic compounds were identified individually by comparison with retention times and mass spectra of authentic standards and NIST library and literature data of mass fragmentation patterns (Medeiros and Simoneit, 2007). For assessing the recoveries, ~100-200 ng of the standard solution was spiked on the blank filter and analyzed as a real sample. Overall, the average recoveries were found to be 80-104% for target compounds. The field and laboratory blank filters (n = 3) were also analyzed by the same procedures as a real sample. Target compounds were not found in the field blanks. The analytical errors based on concentrations by replicate sample analyses (n = 3) were less than 15%.

2.3. Carbon fractions analysis

Organic carbon (OC) and elemental carbon (EC) were analyzed using a thermal-optical transmittance method with a Sunset Laboratory carbon analyzer following the NIOSH protocol (Birch and Cary, 1996), and detailed procedures were given elsewhere (Zhang et al., 2016). Furthermore, a portion of 2.54 cm^2 of each sample filter was extracted with 15 mL ultrapure water (resistivity > 18.2 MΩcm, Sartorius arium 611 UV) with ultrasonication for 30 min. The water extracts were then filtered through a membrane disc filter for water-soluble organic carbon (WSOC) analysis by a total organic carbon (TOC) analyzer (Shimadzu, TOC-Vcsh) (Boreddy et al., 2018). The concentrations of WSOC were corrected by field blanks. The analytical errors in the triplicate analyses were less than 5% for WSOC.

196 **2.4. Radiocarbon isotopic composition of total carbon (TC) and EC**

197 The concentrations of TC in the TSP samples were determined using an elemental analyzer.
198 For the radiocarbon isotopic composition ($\Delta^{14}C$), the aerosol filter punches were exposed for
199 ~12 h to HCl fumes in a vacuum desiccator. Subsequently, these filters were analyzed for
200 $\Delta^{14}C$ on a modified elemental analyzer coupled via a gas interface to Accelerator Mass
201 Spectrometer Mini Carbon Dating System (MICADAS) at the University of Bern,
202 Switzerland (Salazar et al., 2015). The evolved CO_2 of TC from the elemental analyzer was
203 passed through a moisture trap (Sicapent, Merck) and isolated from other residual gasses
204 using a temperature-controlled zeolite trap. The purified CO_2 was introduced through a gas
205 interface system to MICADAS, where $^{14}C/^{12}C$ ratios are measured according to the analytical
206 procedures detailed in Zhang et al. (2016). Likewise, the evolved CO_2 of elemental carbon
207 from the Sunset Lab OC/EC analyzer using the Swiss 4S protocol (Zhang et al., 2012), was
208 directed to the MICADAS and measured for the $^{14}C/^{12}C$ ratio relative to standard calibration
209 gas. These results were expressed as fractions of modern carbon (f_M) by normalizing with a
210 $\delta^{13}C$ value of the reference standard in the year 1950 (–25‰) according to Stuiver and Polach
211 (1997) for the fractionation effects. The f_M(OC) can be estimated by using the f_M(TC) and
212 f_M(EC) in an isotope mass balance equation (Zhang et al., 2015). Additionally, we estimated
213 the relative contributions of OC and EC from the nonfossil and fossil sources ($f_{nonfossil}$ and
214 f_{fossil}, respectively) using the following equations.

215 $$f_{nonfossil\text{-}OC} = f_M(\text{OC-sample})/f_M(\text{OC-ref});\ f_M(\text{OC-ref}) \approx 1.07\pm0.04 \quad (1)$$

216 $$f_{nonfossil\text{-}EC} = f_M(\text{EC-sample})/f_M(\text{EC-ref});\ f_M(\text{EC-ref}) \approx 1.10\pm0.05 \quad (2)$$

217 $$f_{fossil\text{-}OC} = 1 - f_{nonfossil\text{-}OC} \quad (3)$$

218 $$f_{fossil\text{-}EC} = 1 - f_{nonfossil\text{-}EC} \quad (4)$$

219 The reference values of OC and EC were obtained from Mohn et al. (2008). Using
220 the fractions of $f_{fossil\text{-}OC}$ and $f_{nonfossil\text{-}OC}$, we can, therefore, estimate the mass concentration of
221 ambient organic carbon (OC-ambient) from fossil and nonfossil sources (OC_{fossil} and
222 $OC_{nonfossil}$, respectively).

223 $$OC_{nonfossil} = f_{nonfossil\text{-}OC} \times [OC]_{ambient} \quad (5)$$

224 $$OC_{fossil} = f_{fossil\text{-}OC} \times [OC]_{ambient} \quad (6)$$

225 More details on the radiocarbon isotopic composition data over Gosan were reported
226 elsewhere (Zhang et al., 2016).

227 **3. Results and discussion**

3.1. Trajectory and cluster analysis

Backward air mass trajectories are useful for assessing the impact of local versus regional source emissions over Gosan. Seven-day isentropic backward air mass trajectories were computed using the hybrid single-particle Lagrangian integrated trajectory model (HYSPLIT, version 4: Stein et al., 2015) over the KCOG for the sampling period using the meteorological datasets of the Global Data Assimilation System (GDAS) network. The trajectory endpoint files from the HYSPLIT model were further used for the cluster analysis using the Trajstat package (Wang et al., 2009b) for all four seasons (Figure 1). Although cluster analysis revealed the predominance of continental transport in the spring, fall, and winter seasons, the air masses over the KCOG in summer mostly originated from the WNP. Since spring is a transition of winds switching from westerlies to easterlies, Gosan is likely influenced by the long-range transport of dust, pollution, and sea-salt aerosols.

The vertical mixing of pollutants within the boundary layer height also plays an important role in controlling the strength of continental outflow alongside regional meteorology. For instance, the mixing height of air parcels from the HYSPLIT model is mostly confined to 1000 m in winter but somewhat increased towards the spring and fall seasons (Figure S1). This vertical enhancement in the boundary layer height facilitates the transport of mineral dust particles from the arid and semiarid regions in East Asia along with urban pollutants to Gosan in spring and fall compared to winter. However, the strength of the continental outflow somewhat depends on several factors, including source emissions, meteorology, and mixing height of air parcels.

Gosan is influenced by three types of air masses in spring (Figure 1a), from the Mongolian Desert (cluster 1: 15%), North China (cluster 2: 45%), and from the Yellow Sea (cluster 3: 40%). In contrast, the easterlies from the WNP in summer mostly influenced the composition of TSP over the KCOG. This inference is based on the cluster analysis for summer samples (Figure 1b), which showed four regimes, including transport from the Sea of Japan (cluster 1: 13%), WNP (cluster 2: 22%), South China Sea (cluster 3: 46%), and East China Sea (cluster 4: 19%). In contrast, cluster analysis revealed three major transport regimes from East Asia in fall and winter (Figure 1c-d). However, there are subtle differences that exist between winter and fall in terms of influence from nearby versus distant pollution sources. For instance, long-range transport of air masses from west Mongolia (cluster 1: 21%) and the Russian Far East (cluster 3: 14%) exerted a weak influence on the TSP sampled over Gosan in winter. Besides, we observed a somewhat larger impact of air masses from the North China Plain over Gosan (cluster 2: 64%) in winter. In contrast, Gosan is less influenced

by air masses originating from the North China Plain, contributing ~28% (cluster 1) than those from Mongolia (cluster 2: 39%) and the Russian Far East (cluster 3: 33%) in fall. Therefore, the impact of East Asian outflow is stronger in winter than in spring and fall.

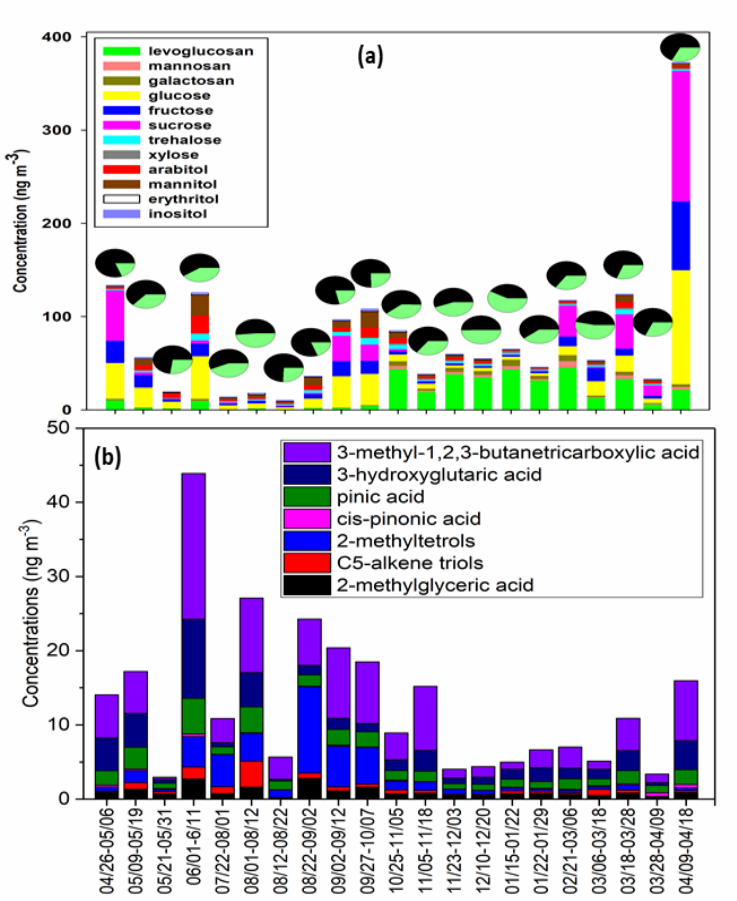

Figure 2. (a) Cumulative concentration levels of anhydrosugars, primary sugars, and sugar alcohols (i.e., represented by bars), and depicting the contributions of nonfossil (green color) and fossil (black color) organic carbon (i.e., pie charts), (b) Cumulative concentration levels of isoprene- and monoterpene-SOA tracers in each TSP sample collected over Gosan.

3.2. Temporal and seasonal variability of sugars

The temporal/seasonal trends of sugar compounds over the KCOG provide useful information on the emission strengths of various sources in the East Asian outflow. All three anhydrosugars showed similar temporal and seasonal trends with higher concentrations in winter and fall than spring and summer (Figures 2a and S2). As levoglucosan and other two anhydrosugars (mannosan and galactosan) are the pyrolysis products of cellulose/hemicellulose, their higher concentrations along with an increase in nonfossil

fraction of OC (Figure 2a; pie charts) in TSP from winter and fall revealed the impact of BB emissions. The MODIS satellite-based fire counts (Figure S1) together with cluster analysis in winter and fall (Figure 1) have revealed an influence of active BB emissions in the North China Plain, Mongolia, and the Russian Far East. The temporal trends of glucose, fructose, and sucrose exhibited less variability throughout the sampling period; however, we observed a slight increase in their concentration towards spring/summer (Figure 2a). Glucose and fructose have origins from leaf fragments and pollen species (Fu et al., 2012a). Sucrose is a potential tracer for airborne pollen (Fu et al., 2012a) and late spring/early summer is often regarded as a season of "pollen-allergies". Therefore, the similar temporal trends of glucose and fructose with sucrose indicate their common source, pollens (Figure 2a). Since glucose, fructose, and sucrose showed moderately significant correlations (R^2 = 0.44-0.48, $p<0.01$) with levoglucosan in winter, it is somewhat possible that BB source emission could also influence the concentrations of these saccharides in this season (Haque et al., 2019; Fu et al., 2008).

BB also contributes to xylose and, hence, the temporal variability of xylose is mimicking that of the anhydrosugars. Trehalose is a primary sugar and a useful tracer for organic carbon associated with soil dust particles (Fu et al., 2012a). The temporal variability of trehalose closely resembled that of the fungal spore tracers (arabitol, mannitol, and erythritol), showing high concentrations in the spring, summer, and fall seasons (Figures 2a and S2) (Zhu et al., 2015a; Fu et al., 2012a). The KCOG is under the influence of a large-scale advection of mineral dust from East Asia to the WNP during these three seasons (Tyagi et al., 2017; Huebert et al., 2003). The mineral dust transport from East Asia to the WNP can be traced by the high concentrations of non-sea-salt Ca^{2+} in the TSP samples from Gosan (Arimoto et al., 1996). Similar temporal trends of trehalose and nss-Ca^{2+}, particularly in spring samples (Figure S3), suggest that the abundance of OA specific to fungal spores over Gosan is likely associated with the Kosa (Asian dust) events.

The major sources of arabitol and mannitol are airborne fungal spores (Bauer et al., 2008), accompanying detritus from mature leaves (Pashynska et al., 2002). Heald and Spracklen (2009) reported that mannitol and arabitol are considerably associated with terrestrial biosphere activity. Inositol is largely derived from the developing leaves in summer (Pashynska et al., 2002) and BB in winter (Fu et al., 2010b). Zhu et al. (2015b) found a similar seasonal behavior of inositol with those of other sugar alcohols with the predominance in summer, associated with microbial activities in local forests from Okinawa. Inositol showed a moderately significant correlation with levoglucosan (R^2 = 0.33, $p< 0.01$)

in winter; however, there were no positive linear relationships between levoglucosan and other sugar alcohols, implying a partial emission of inositol from the BB during winter in Gosan aerosols. Therefore, the temporal variability of inositol differs from that of the other sugar alcohols (Figure S2). The sources of sugar compounds are further discussed in section 3.4.

The seasonally averaged concentrations of all the anhydrosugars and xylose are higher in winter/fall than spring/summer (Figure 3a-d), possibly due to a greater influence of long-range transport from East Asia. In contrast, glucose, fructose, and sucrose peaked in spring but decreased in the other seasons (Figure 3e-g), mainly because of the contribution of airborne pollen. Trehalose showed higher concentrations in fall and summer, followed by spring and winter (Figure 3h). Arabitol, mannitol, and erythritol showed higher concentrations in summer/fall than in winter and spring (Figure 3i-k). This seasonal trend is consistent with those of soil-derived fungal spores. This feature is consistent with earlier observations from a remote oceanic island in the WNP (Okinawa) during the impact of East Asian outflow (Zhu et al., 2015a). The seasonally averaged mass concentrations of inositol are highest in spring, followed by summer, fall, and winter (Figure 3l). Overall, the molecular compositions of anhydrosugars showed the predominance of levoglucosan followed by galactosan and mannosan (Figure S4). Galactosan is more abundant in crop-residue burning emissions than mannosan (Engling et al., 2009; Sheesley et al., 2003). It is very much likely that the impact of crop-residue burning emissions in East Asia over Gosan is more prominent in winter/spring. Such high abundances of galactosan over mannosan were found in the North China Plain (Fu et al., 2008) and in the Indo-Gangetic Plain outflow sampled over the Bay of Bengal (Bikkina et al., 2019). Although the temporal variability of primary sugars in the TSP samples from Gosan showed a characteristic peak of glucose and sucrose (Figure 2a), the seasonally averaged distributions are different (Figure S4). The molecular distributions of sugar alcohols are characterized by high loadings of arabitol and mannitol, followed by erythritol and inositol (Figure S4).

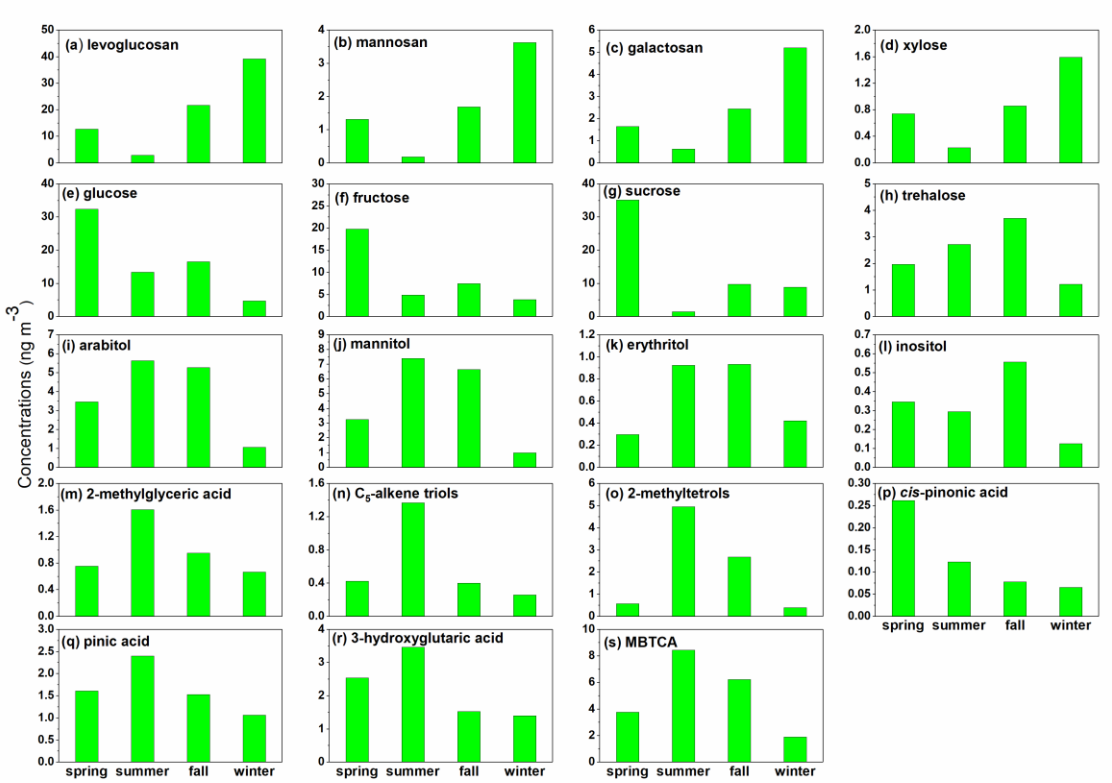

Figure 3. Seasonal variability of the atmospheric levels of sugar compounds and BSOA tracers in TSP samples from Gosan during April 2013-April 2014.

3.3. Temporal and seasonal variability of BSOA tracers

We identified six isoprene-SOA tracers such as 2-methylglyceric acid (2-MGA), three C_5-alkene triols, and two 2-methyltetrols (2-methylthreitol and 2-methylerythritol) (2-MTs) in Gosan aerosol samples (Table 1). The sum of the isoprene-SOA tracers ranged from 0.35 to 15.1 ng m^{-3} (avg. 3.69 ng m^{-3}) with the predominance of 2-MTs (avg. 2.09 ng m^{-3}). 2-MGA is the second most abundant isoprene-SOA tracer (avg. 0.99 ng m^{-3}), a high-generation product probably formed by further photooxidation of methacrolein and methacrylic acid. A similar molecular composition was observed over the North Pacific and California Coast (Fu et al., 2011). All the isoprene-SOA tracers exhibited similar temporal variations with higher concentrations in the summer/spring months compared to autumn and winter (Figure 2b). Conversely, four monoterpene-SOA tracers, i.e., *cis*-pinonic acid, pinic acid, 3-hydroxyglutaric acid (3-HGA), and 3-methyl-1,2,3-butanetricarboxylic acid (MBTCA), were detected in the Gosan samples (Table 1). The total concentrations of monoterpene-SOA tracers were found to be 1.65 to 35.5 ng m^{-3} (avg. 9.24 ng m^{-3}) with a high concentration of MBTCA (avg. 5.11 ng m^{-3}). All the monoterpene-SOA tracers showed similar temporal trends with high values in summer/spring periods than autumn/winter (Figure 2b).

Nevertheless, *cis*-pinonic acid was ascribed a somewhat different temporal variability with other monoterpene-SOA tracers. It is likely that *cis*-pinonic acid might be further photo-oxidized to form MBTCA (Szmigielski et al., 2007).

The seasonal average of isoprene-SOA tracers showed high concentrations in summer, followed by spring/fall and winter (Figure 3m-o). One key feature of the data presented here is that two fall samples (KOS984; 2-12 September and KOS986; 27 September to 07 October) exhibited high concentrations for 2-MTs over Gosan (Figure 2b). We presumed that local vegetation might contribute significantly to the formation of 2-MTs as it is a first-generation product. Moreover, 2-MTs can be derived from the open ocean under low NO_x conditions (Hu et al., 2013). 3-HGA and pinic acid showed somewhat higher concentrations in summer/spring than fall/winter due to the growing vegetation (Figure 3q-r). *Cis*-pinonic acid was more abundant in spring compared to summer (Figure 3p) because of its photo-degradation, as discussed above. In contrast, MBTCA was dominant in summer/fall than spring/winter (Figure 3s). Here, the formation of MBTCA could be enhanced in fall during atmospheric transport from East Asia. The molecular distributions of isoprene-SOA tracers were characterized by a high loading of 2-MTs, followed by 2-MGA and C_5-alkene triols in all seasons (Figure S4). The molecular composition of monoterpene-SOA tracers was dominated by MBTCA, followed by 3-HGA, pinic acid, and *cis*-pinonic acid in all seasons (Figure S4). Overall, BSOA tracers were found to be most abundant in summer, followed by fall, spring, and winter (Table 1). Interestingly, it is likely that secondary OA undergoes much faster cycling than the primary sugar compounds, considering the feasibility of photooxidation. This would mean a slight underestimation of BSOA over the KCOG in the East Asian outflow and, hence, their atmospheric abundances over Gosan reflect a lower limit.

Kang et al. (2018b) reported that monoterpene-SOA tracers were more abundant than isoprene-SOA tracers in spring-summer over the East China Sea, which is consistent with this study. Although the mass budget calculations showed that isoprene and monoterpenes are largely emitted by terrestrial plants; however, the open ocean can also contribute to isoprene and monoterpenes significantly (Conte et al., 2020; Shaw et al., 2010; Broadgate et al., 1997). Air mass back trajectory and cluster analysis (Figure 1) implied that the air masses mostly originated from the ocean during summer. This means the open ocean significantly contributed to isoprene-SOA production. However, terrestrial sources from the continent also substantially enhanced the formation of BSOA. For example, one sample (KOS979; 1-11

June 2013) during summer showed the highest loading of BSOA tracers (Figure 2b) when air masses were transported from the continent (Zhang et al., 2016).

Figure 4. Multiple linear regression (MLR) analysis of airborne sugar compounds in TSP collected over Gosan.

3.4. Source apportionment- regression analysis and diagnostic ratios

Anhydrosugars strongly correlated with xylose (Figure 4), suggesting their common source as BB emission in East Asia. Fu et al. (2012a) analyzed pollen from different tree species (*e.g.*, White birch, Chinese willow, Peking willow, Sugi, Hinoki), which are enriched in sucrose (182-37,300 μg g^{-1}), glucose (378-3601 μg g^{-1}) and fructose (162-1813 μg g^{-1}). In our samples, sucrose strongly correlated with glucose and fructose (Figure 4), suggesting their origin from plant-derived airborne pollen. Likewise, a strong correlation was found between arabitol and mannitol, indicating a mutual origin from a similar type of fungal spores (Zhu et al., 2015a; Fu et al., 2012a; Bauer et al., 2008; Yttri et al., 2007). Bauer et al. (2008) ascribed

weak correlations between arabitol and mannitol to the diverse nature of ambient fungal spores. Furthermore, both sugar alcohols correlated well with trehalose, a tracer for soil organic carbon (Fu et al., 2012a). This observation suggests their common origin from soil organic matter associated with fungal spores. Erythritol also originates from fungal spores; however, its abundance is affected by the atmospheric aging process. Kessler et al. (2010) reported that erythritol is degraded during long-range transport in 12.7 days. Consequently, arabitol and mannitol were moderately correlated with erythritol in the Gosan samples due to the degradation of the latter sugar alcohol in the East Asian outflow.

The linear relationship of levoglucosan (*Lev*) with mannosan (*Man*), galactosan (*Gal*), and nss-K^+ provide useful information on the type of BB emissions (hardwood, softwood, or crop-residue). Ratios of *Lev*/*Man* and *Lev*/(*Man* + *Gal*) can be useful to distinguish BB and coal combustion contributions. The average ratios of *Lev*/*Man* (15.1 ± 6.76) and *Lev*/(*Man* + *Gal*) (4.27 ± 1.23) in Gosan aerosols are much closer to those from wood burning and coal combustion sources emissions, respectively (Yan et al., 2018). It reveals that *Lev* could originate from both biomass and coal burning source emissions, which is consistent with the linear relationship between *Lev*-C and the fossil-/nonfossil carbon fraction (section 3.6). Furthermore, different types of biomass are characterized by distinct *Lev/Man* ratios. For instance, *Lev/Man* ratios from the softwood burning emissions (3-10) differ from those of hardwood (15-25) and crop-residues (>40) (Singh et al., 2017; Schmidl et al., 2008a, b; Fu et al., 2008; Engling et al., 2006, 2009; Fine et al., 2001, 2004). We found that the *Lev/Man* ratios (Table 2) over the KCOG overlap between seasons and are somewhat close to that of hardwood burning emissions in northern China, Mongolia, and the Russian Far East, as corroborated by the backward air mass trajectories and MODIS fire counts (Figures 1 and S1). Besides, *Lev*/K^+ and *Man/Gal* ratios in summer differ from those of other seasons (Table 2). Cheng et al. (2013) have apportioned qualitatively the source contributions of anhydrosugars over a receptor site based on the comparison of *Lev*/K^+ and *Lev/Man* ratios in aerosols to those from various sources profiles compiled from the literature. This approach of using the mass ratios of *Lev/Man* and *Lev*/K^+ has been proven useful for deciphering the difference in BB-derived OA (Bikkina et al., 2019).

Here, we adopted this methodology to ascertain the likely contributing sources of anhydrosugars, which are BB tracers from different seasons (Figure 5). This source apportionment relies on the fact that the *Lev*/K^+ ratio from the softwood burning (10-1000) is higher than from hardwood (1-100) (Fine et al., 2004). In contrast, *Lev*/*Man* ratios for softwood are lower than those of hardwood burning (10-100) (Fine et al., 2004). Likewise,

the *Lev/Man* and *Lev*/K^+ ratios from grasses and crop-residues are 10-100 and 0.01-1.0, respectively (Bikkina et al., 2019). On a similar note, the *Lev*/K^+ ratios from the burning of pine needles (0.1-1.0) somewhat overlap with those from hardwood burning emissions but are characterized by distinct *Lev/Man* ratios (Bikkina et al., 2019). The burning of dead leaves (duff) showed higher *Lev*/K^+ ratios than those of pine needles and grasses, but their *Lev/Man* ratio is on the lower side than for the former biomass type and the softwood burning emissions. However, *Lev* is more susceptible to degradation by photooxidation with OH radicals during atmospheric transport (half-life: <2.2 days) (Hennigan et al., 2010) and this would cause lower abundances of this anhydrosugar. Hence, the hardwood *Lev*/K^+ ratios could slightly shift downwards. Therefore, caution is required while interpreting the ambient data from a receptor site (Bikkina et al., 2019). Overlapping the seasonal data on this scatter plot of *Lev*/K^+ versus *Lev/Man* (Figure 5) clearly revealed a mixed contribution of burning of hardwood and crop-residue in the East Asian outflow. It should be noted that the photooxidation process during atmospheric transport is also applicable for low concentrations and poor correlations of other primary saccharides.

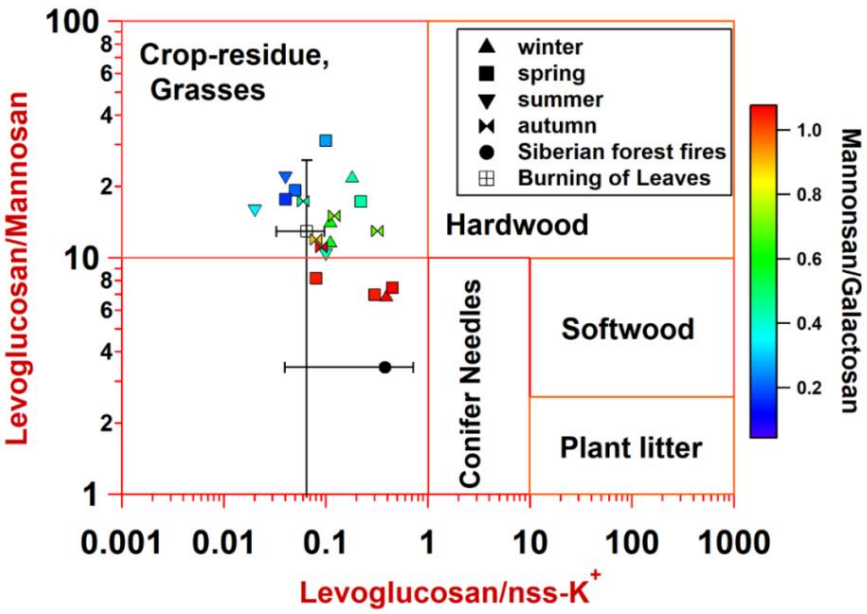

Figure 5. Scatter plot of levoglucosan/K^+ versus levoglucosan/mannosan ratios in TSP collected over Gosan during April 2013-April 2014. The data for Siberian forest fires and burning leaves were adopted from Sullivan et al. (2008).

The correlation coefficients and diagnostic ratios of BSOA tracers specify their source origin or formation pathway. Nevertheless, atmospheric stability or reactivity of BSOA tracers through the photooxidation during long-range transport may bias the correlation coefficients in Gosan aerosols. 2-MGA showed a significant correlation with 2-MTs ($r = 0.79$, $p<0.01$) and C_5-alkene triols ($r = 0.50$, $p<0.05$) (Figure 6a-b), suggesting their similar formation pathway or common sources of isoprene-SOA tracers. However, a poor correlation coefficient between 2-MTs and C_5-alkene triols ($r = 0.33$, $p = 0.13$) (Figure 6c) indicates their different formation process over the Gosan atmosphere. Wang et al. (2005) documented that polyols are formed from isoprene through diepoxy derivatives, which further convert into 2-MTs by acid-catalyzed hydrolysis. On the other hand, C_5-alkene triols are produced from the precursor of hydroxyperoxy radicals that are initially derived from isoprene through rearrangement reactions (Surratt et al., 2006). It can be noted that the formation mechanisms of 2-MGA and 2-MTs are different while depending on the NO_x concentrations (Surratt et al., 2010). Thus, the ratio of 2-MGA/2-MTs attributes to the influence of NO_x on isoprene-SOA formation. We found a low ratio of 2-MGA/2-MTs (0.67) (Figure S5a, Table 2) in summer, implying enhancement of 2-MTs formation over the open ocean due to the low-NO_x environment in the ocean atmosphere. On the contrary, the 2-MGA/2-MTs ratios for other seasons were >1.0 (Figure S5a, Table 2), indicating an elevated formation of 2-MGA through continental high NO_x condition, which is consistent with the air masses back trajectory.

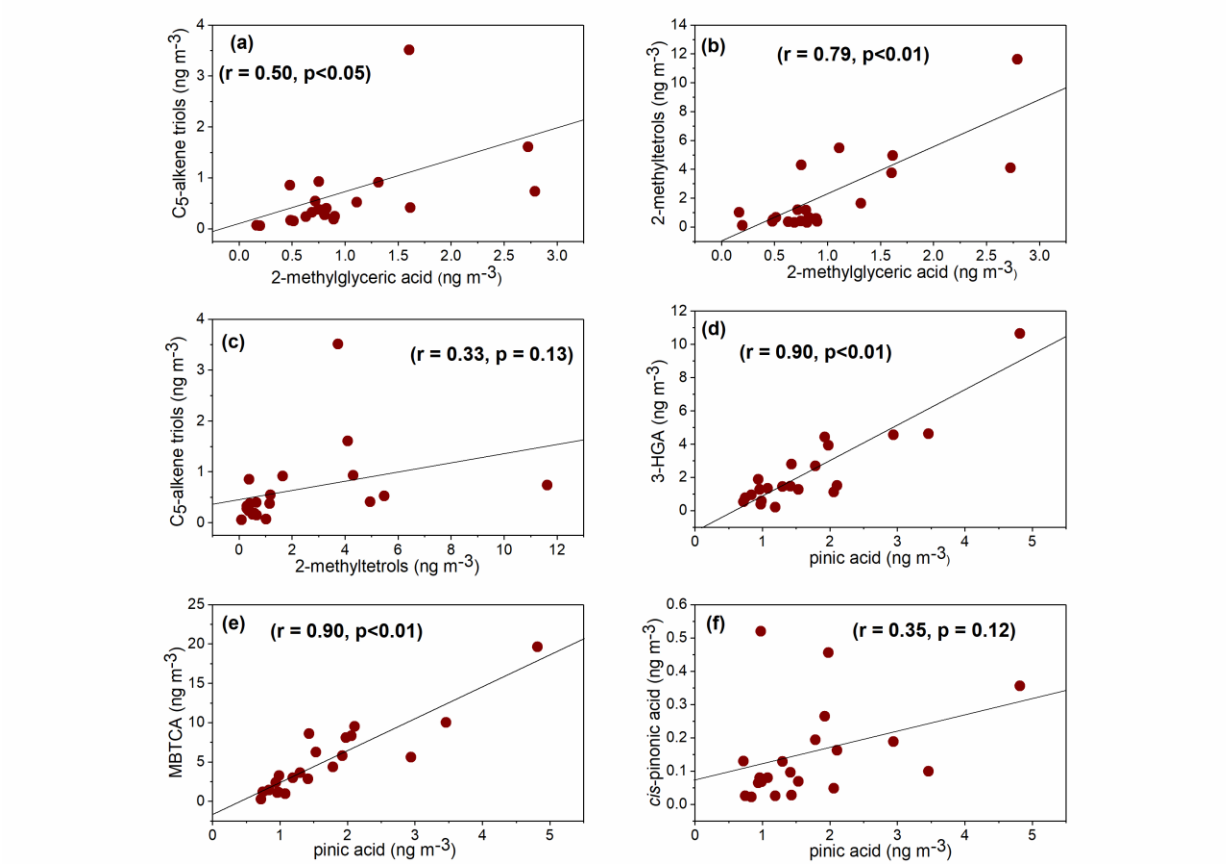

506

507 **Figure 6.** Pearson linear correlation coefficient analysis of BSOA tracers in Gosan TSP
508 aerosols during April 2013-April 2014.

509

510 *Cis*-pinonic acid showed a weak correlation with pinic acid (r = 0.35, p = 0.12)
511 (Figure 6f), suggesting that different atmospheric reactivity of cis-pinonic/pinic acids during
512 transport would cause such poor correlation. In contrast, pinic acid exhibited a strong positive
513 linear correlation with 3-HGA (r = 0.90, p<0.01) and MBTCA (r 0.90, p<0.01) (Figure 6d-e),
514 implying their similar sources. It should be noted that the formation processes of pinic acid,
515 3-HGA, and MBTCA are different because pinic acid is a first-generation product, and 3-
516 HGA and MBTCA are high-generation products (Claeys et al., 2007; Müller et al., 2012;
517 Szmigielski et al., 2007). The ratio of *cis*-pinonic acid + pinic acid to MBTCA (P/M) is used
518 to evaluate the aging of monoterpene-SOA.

519 A low P/M ratio suggests the transformation of *cis*-pinonic and pinic acids to
520 MBTCA and thus relatively aged monoterpene-SOA, whereas a high ratio reflects relatively
521 fresh monoterpene-SOA (Gómez-González et al., 2012; Ding et al., 2014). Gómez-González
522 et al. (2012) reported aged monoterpene-SOA (P/M = 0.84) from a Belgian forest site while
523 fresh chamber-produced α-pinene-SOA tracers showed P/M ratios of 1.51 to 3.21 (Offenberg

et al., 2007). The average ratio of P/M in this study showed 0.62 with the low value in summer (Figure S5b, Table 2), which is lower than those of Guangzhou (fresh monoterpene-SOA; 28.9) while the air masses originated from southern China (Ding et al., 2014). This observation indicates that monoterpenes SOA have undergone substantial aging during transport to Gosan, particularly in summer when extensive photochemical oxidation occurred due to the high temperature and intense solar radiation.

3.5. Relative abundances in WSOC and OC

Levoglucosan is the most abundant anhydrosugar, contributing 0.05-1.54% of WSOC and 0.03-1.02% of OC. Likewise, sucrose, glucose, and fructose were more abundant primary sugars, contributing 0.01-2.83%, 0.03-1.22%, and 0.02-0.74% of WSOC, respectively. Contributions of the three primary sugars varied from 0.05% to 3.41% of OC. Arabitol and mannitol are the most abundant sugar alcohols, whose contribution to WSOC and OC ranged from 0.02% to 0.93% and 0.01% to 0.85%, respectively. Figure 7 depicts the contribution of sugar compounds to WSOC and OC in TSP collected over Gosan during the study period. We also compared the atmospheric abundances of sugar compounds from Gosan with the literature data (Table 3). This comparison revealed the less influence of BB tracer compounds (i.e., anhydrosugar levels) over Gosan, a factor of 5-10 times lower than those reported for the BB-influenced source regions in China and East Asia (Fu et al., 2012b; Kang et al., 2018a; Wang and Kawamura, 2005; Wang et al., 2012). However, the levels of anhydrosugar over Gosan are higher than those observed over the remote Canadian High Arctic site (Fu et al., 2009a). In contrast, Gosan is characterized by high concentrations of primary sugars compared to other remote sampling sites in Table 3. This is because of the overwhelming contribution of primary sugars associated with soil dust particles over Gosan during the East Asian outflow. Such high loadings of primary sugars were observed from other remote island receptor sites in the WNP (Okinawa) during the spring season (Zhu et al., 2015a). Likewise, the concentrations of sugar alcohols from Gosan are similar to those from other receptor sites influenced by the East Asian outflow (Verma et al., 2018; Zhu et al., 2015a).

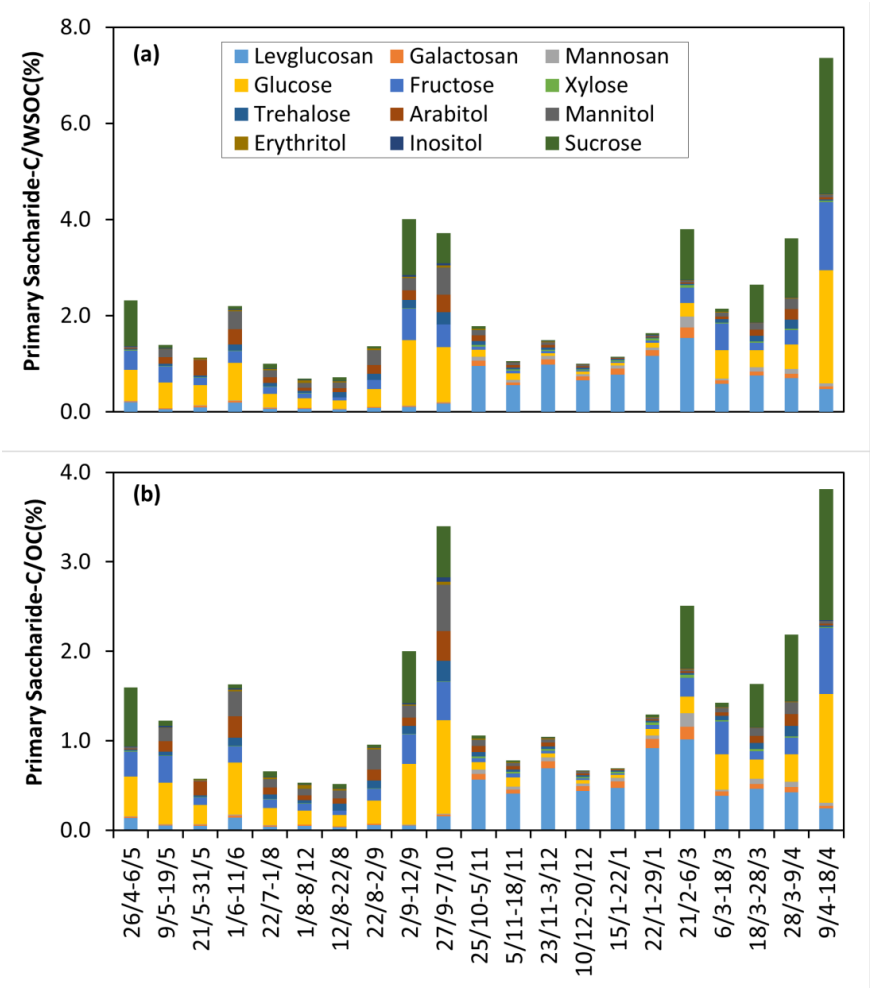

555

556 **Figure 7.** Contribution of primary saccharide-C in (a) WSOC(%) and (b) OC(%) in TSP
557 collected over Gosan during April 2013-April 2014.

558

559 The Contributions of isoprene-SOA tracers to ambient OC (0.01-0.40%, avg. 0.09%)
560 and WSOC (0.02-0.57%, 0.13%) were lower than those of monoterpene-derived SOA (0.04-
561 0.63%, 0.23% for OC and 0.06-0.82%, 0.33% for WSOC). The contributions of isoprene
562 oxidation products to OC and WSOC were found to be highest in summer (0.23% and 0.32%,
563 respectively), followed by fall (0.09% and 0.13%), spring (0.04% and 0.06%), and winter
564 (0.02% and 0.03%). Likewise, the contributions of monoterpene-SOA products to aerosol OC
565 and WSOC exhibited the highest value in summer (0.40% and 0.55%, respectively), followed
566 by fall (0.24% and 0.35%), spring (0.18% and 0.27%), and winter (0.10% and 0.14%). We
567 found that the contribution of BSOA products to the carbonaceous components was twice in
568 summer (Figure 8, Table 2). This means BSOA formation occurred in summer to a greater
569 extent due to the intensive BVOCs emission with key factors of meteorological parameters
570 (higher temperature and radiation), i.e., higher concentrations of ozone, and other oxidizing

agents (NO_x, OH, etc.). It should be pointed out that the fraction of WSOC in OC (WSOC/OC) is often prone to photochemical aging and, hence, contributes to SOA. More specifically, the WSOC/OC > 0.4 over a receptor site indicates aged aerosols with a significant SOA contribution (Haque et al., 2019; Boreddy et al., 2018). In our study, the average WSOC/OC ratio was observed 0.68 with the highest in summer (0.72), although subtle difference exhibited in winter/autumn (> 0.68), implying the presence of aged OA over the KCOG. Such higher abundances of SOA over Gosan during transport from East Asia is mainly due to photochemical aging of anthropogenic (fossil fuel/biomass combustion) emissions. Huang et al. (2014) reported significant SOA formation from the fossil fuel/biomass combustion precursor VOCs in winter over China.

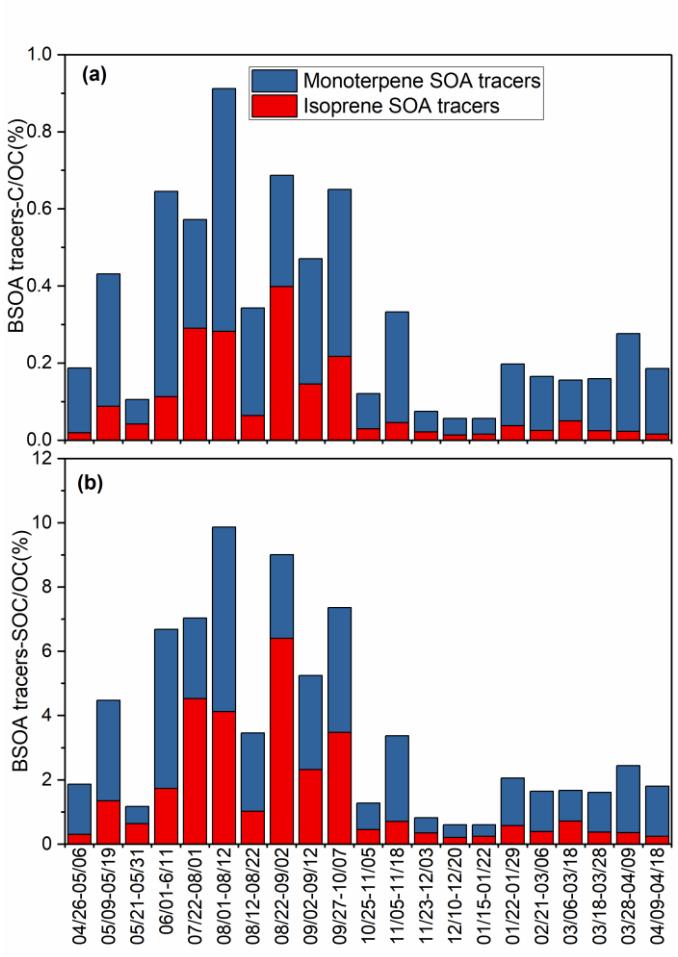

Figure 8. Contribution of (a) isoprene- and monoterpene-SOA tracers-C in ambient OC(%) and (b) isoprene- and monoterpene-SOA tracers-SOC in ambient OC(%) in Gosan aerosol samples during April 2013-April 2014.

We estimated secondary organic carbon (SOC) derived from isoprene and monoterpenes, using the measured values of BSOA tracers and following the SOA tracer-based method first proposed by Kleindienst et al. (2007). A summary of the estimated SOC is provided in Table 2. The contribution of isoprene to SOC was calculated 2.26 to 97.4 ngC m^{-3} (avg. 23.7 ngC m^{-3}), accounting for 1.45% of OC and 35.5% of total BSOC with the predominance in summer (3.56% and 46.6% for OC and SOC, respectively). The estimation of monoterpene-SOA to SOC (avg. 40.1 ngC m^{-3}) was observed around two times higher than that of isoprene-SOA (Table 2). Interestingly, the contribution of monoterpene-derived SOC to ambient OC (3.65%) was dominant in summer, but monoterpene SOC to total SOC (72.1%) was most abundant in spring (Figure 8b). The seasonal distributions of biogenic SOC (Table 2) implied that a substantial amount of SOC was formed from monoterpenes in spring. The estimated biogenic SOC at the KCOG is almost one order of magnitude lower than those from other continental sites in China urban areas (e.g., Pearl River Delta: 446 ngC m^{-3}) (Ding et al., 2012). However, the estimated biogenic SOC load from the KCOG is much higher than that reported from a remote site in the Canadian High Arctic (Alert: 9.4 ngC m^{-3}) (Fu et al., 2009b) and comparable with over the East China Sea (Kang et al., 2018b).

It should be noted that concentrations of SOA tracers cannot always provide the actual contribution of the biogenic source to ambient organic aerosol mass. For example, loadings of monoterpene-SOA tracers were lower in sample KOS999 (28 March - 9 April 2014) (3.02 ng m^{-3}) compared to sample KOS1000 (9 - 18 April 2014) (14.4 ng m^{-3}), whereas the estimated contribution of SOC to ambient OC showed an opposite trend (KOS999: 2.08%; KOS1000: 1.56%). This result demonstrates that the estimation of SOC is an important factor in evaluating the contribution of BSOA to organic aerosol mass. We calculated biogenic OC using radiocarbon (^{14}C) data following the method proposed by Szidat et al. (2006). Biogenic OC showed a poor correlation with biogenic SOC ($r = 0.36$, $p = 0.09$) but a significant linear relationship with primary sugars (i.e., glucose, fructose and sucrose) ($r = 0.54$, $p<0.5$), suggesting that primary bioaerosols from plant-derived airborne pollen dictate on biogenic OC over Gosan.

3.6. Significance of fossil fuel as a source for levoglucosan

The ambient *Lev* levels showed a significant linear relationship with the OC_{fossil}, suggesting the fossil source contribution of this molecular marker (Figure 9a). However, such a significant correlation was not evident between OC_{fossil} and other major sugar compounds. Until recently, *Lev* has been thought to originate primarily from the hemicellulose/cellulose pyrolysis of vegetation and, hence, can be employed as a powerful tracer for biomass smoke

621 particles (Fraser and Lakshmanan, 2000; Simoneit et al., 1999). Nevertheless, residential
622 coals (*e.g.,* lignite and bituminous coal) have been shown to contain high concentrations of
623 '*Lev*' but also emit traces of *Man and Gal* (Kourtchev et al., 2011; Fabbri et al., 2008).
624 Recently, Yan et al. (2018) found a significant linear relationship between the ^{14}C-based
625 fossil fraction of WSOC and *Lev-C* in the aerosols generated from coal combustion and the
626 ambient aerosol samples. Therefore, the prevailing linear relationship between OC_{fossil} and
627 *Lev*-C in the Gosan samples (Figure 9a) is likely due to a common source contribution from
628 coal combustion in East Asia.

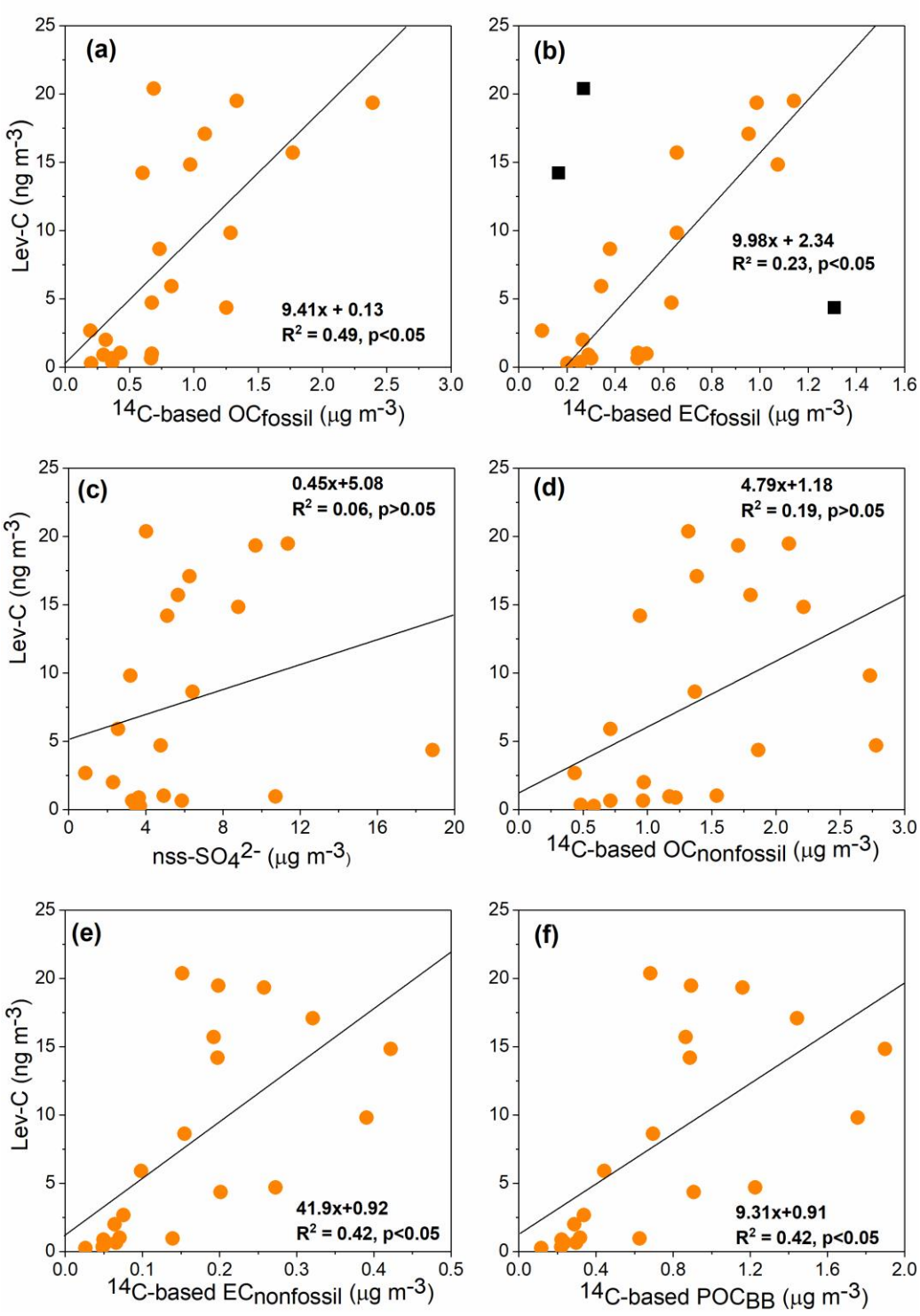

Figure 9. Linear regression analysis between levoglucosan in terms of their carbon content (*Lev*-C) and ^{14}C-based mass concentrations of (a) organic carbon and (b) elemental carbon of fossil origin (OC_{fossil} and EC_{fossil}, respectively), (c) nss-SO_4^{2-}, (d) nonfossil derived organic carbon ($OC_{nonfossil}$), (e) nonfossil derived elemental carbon ($EC_{nonfossil}$), and (f) biomass burning derived primary OC (POC_{BB}) in TSP collected over Gosan during April 2013-April 2014. In panel (b), the squares represent three outliers (i.e., samples with rather high and low *Lev*/EC ratios; please see text for more details).

637 The slope of the linear regression between *Lev-C* and OC_{fossil} (0.0094; Figure 9a) is
638 higher than those documented for the coal combustion source in China (~0.004±0.007) (Yan
639 et al., 2018). Moreover, *Lev-C* moderately correlated with the EC_{fossil} with the regression
640 slope (~0.01) in the Gosan samples (Figure 9b), being comparable to that observed for the
641 coal combustion in China (0.044±0.076) (Yan et al., 2018). It should be noted that excluding
642 the three outliers as shown in Figure 9b (black square), *Lev-C* showed a stronger correlation
643 with EC_{fossil} (R^2 = 0.74, $p < 0.05$). Of these, two outliers in winter (KOS995: 22-29 January
644 2014; KOS996: 21 February - 3 March 2014) have higher *Lev*-C levels over that of EC_{fossil},
645 when air mass trajectories showed the impact of BB emissions in the North China Plain. In
646 contrast, the third outlier in summer (KOS979: 1-11 June 2013) has a lower *Lev*-C/EC_{fossil},
647 while air parcels transported from nearby cities in China, Korea, and Japan, thus, have more
648 contribution from vehicular emissions. Overall, both the regression slopes are, thus, the
649 representative nature of *Lev*-C/OC_{fossil} and *Lev*-C/EC_{fossil} in the East Asian outflow. *Lev*-C and
650 nss-SO_4^{2-} exhibited a poor correlation (Figure 9c), although both were transported from East
651 Asia.

652 *Lev*-C exhibited a rather weak correlation with $OC_{nonfossil}$ (R^2 = 0.19) than that with
653 $EC_{nonfossil}$ (R^2 = 0.42) over Gosan during the study period (Figure 9d-e). This could be likely
654 because $OC_{nonfossil}$ has contributions from the BB and the secondary formation process or the
655 primary biogenic sources. The contribution of primary OC generated from BB (POC_{BB}) to
656 $OC_{nonfossil}$ was taken from Zhang et al. (2016). In their study, the ^{14}C-based $EC_{nonfossil}$ levels
657 were scaled by a factor to constrain the POC_{BB} (Zhang et al., 2016). Here the conversion
658 factor is '4.5' (range: 3-10), which is a median value representing the primary OC/EC ratio
659 from BB emissions ($(POC/EC)_{BB}$).

660 $$POC_{BB} = EC_{nonfossil} \times (POC/EC)_{BB} \quad (7)$$

661 *Lev*-C showed a somewhat improved linear correlation with POC_{BB} than with the $OC_{nonfossil}$
662 (Figure 9f). It is apparent from Figure 9 that the regression slopes are comparable, indicating
663 their contribution to *Lev* from both coal combustion and BB emissions over Gosan. The
664 prevailing weak linear relationship (moderate correlation) of *Lev* with nonfossil and fossil
665 carbon fractions is likely the result of photo-degradation of *Lev* during atmospheric transport.
666 This result would mean that the higher atmospheric abundance of *Lev* and its pronounced
667 linear relationships with the nonfossil and fossil carbon fractions implies a much stronger
668 impact of both source emissions in East Asia during the continental outflow in winter and
669 spring.

Overall, we present a new finding on the contribution of coal combustion sources in East Asia in controlling the atmospheric levels of *Lev* apart from the traditional biomass/biofuel burning emissions. This is based on the prevailing linear relationship between the radiocarbon based nonfossil-EC and *Lev* in the year-round TSP samples collected from the KCOG site in Jeju Island. The Gosan supersite is the best location to understand how the chemical composition of source-emissions from East Asia affects the outflow regions in winter and spring. Recent studies have highlighted the potential contribution of *Lev* from residential coal combustion in China (Yan et al., 2018), with estimated annual emission of ~2.2 Gg of *Lev* from domestic coal combustion (Wu et al., 2021). Given this background information, the prevailing significant linear relationship between *Lev* and nonfossil-EC (p-value < 0.05) over the KCOG clearly emphasizes the need for reconsideration of the previous assessments on the impact of BB in East Asian outflow to the WNP. Additionally, this dataset is further compared with the molecular distributions and relative abundances of organic tracers in the TSP samples collected over Gosan during 2001, a decade ago (Fu et al., 2012a). This comparison allows us to better understand the regional changes in the emission sources (*e.g.,* fugitive dust, BB, and fossil-fuel combustion) on a decadal basis.

4. Conclusions

We investigated seasonal variations of primary organic components such as anhydrosugars, primary sugars, and sugar alcohols and biogenic secondary organic aerosol (BSOA) tracers (isoprene- and monoterpene-derived SOA products) in ambient aerosols from Gosan, Jeju Island. Among the detected sugar compounds, levoglucosan was dominant in winter/fall, whereas glucose and sucrose were more abundant in spring/summer. The seasonal trends documented that BB impact is more significant in winter/fall and the primary bioaerosol particles are important in spring/summer. Diagnostic ratios of levoglucosan, galactosan, and mannosan reflect that emissions from BB are mostly dominated by hardwood. The significant linear relationship of sucrose with glucose and fructose suggests their origin from airborne pollen. On a similar note, trehalose showed a significant positive correlation with arabitol, mannitol, and erythritol, implying their contribution from airborne fungal spores and soil microbes over the KCOG.

Distributions of biogenic SOA tracers were characterized by a predominance of monoterpene- than isoprene-derived oxidation products in Gosan aerosols. The BSOA tracers were formed in summer to a greater extent, followed by fall/spring and then winter. The low ratio of *cis*-pinonic acid + pinic acid to MBTCA (P/M) demonstrated that monoterpene-SOA

was relatively aged over Gosan aerosols. The estimated secondary organic carbon (SOC) with the predominance in summer shows that substantial BSOA formation occurred in summer due to favorable meteorological conditions. The backward air mass trajectories and source apportionment studies entirely demonstrated that emission from East Asia significantly dominates the ambient OA mass over KCOG. Interestingly, levoglucosan-*C* exhibited a significant positive correlation with nonfossil and fossil organic carbon fractions, along with the comparable regression slopes. This result reveals that BB and coal (lignite) combustion both are prominent sources for levoglucosan in the East Asian outflow.

Although there is some evidence that levoglucosan could originate from the combustion of brown coals (*e.g.*, lignite) in China, our observations from the KCOG (receptor site) also hinted at the fossil source contribution of this molecular marker in the regional influx of the East Asian outflow. Therefore, attribution of ambient levoglucosan levels over the WNP to the impact of BB emission may cause large uncertainty.

Data availability

The data used in this paper are available upon request from the corresponding author.

Author contributions

KK and YLZ designed the research. ML collected the aerosol samples. MMH and SB performed the analysis of aerosol samples. MMH wrote the paper under the guidance of YLZ and KK. All authors were actively involved in the discussion of the paper.

Competing interests

The authors declare that they have no conflict of interest.

Acknowledgments

We acknowledge the financial supports of the Japan Society for the Promotion of Science (JSPS) through Grant-in-Aid No. 24221001 and the National Natural Science Foundation of China (Grant No 41977305).

References

Arimoto, R., Duce, R. A., Savoie, D. L., Prospero, J. M., Talbot, R., Cullen, J. D., Tomza, U., Lewis, N. F., and Ray, B. J.: Relationships among aerosol constituents from Asia and the North Pacific during PEM-West A, J. Geophys. Res. Atmos., 101, 2011-2023, https://doi.org/10.1029/95JD01071, 1996.

Athanasopoulou, E., Tombrou, M., Russell, A. G., Karanasiou, A., Eleftheriadis, K., and Dandou, A.: Implementation of road and soil dust emission parameterizations in the aerosol model CAMx: Applications over the greater Athens urban area affected by natural sources, J. Geophys. Res., 115, D17301, https://doi.org/10.1029/2009JD013207, 2010.

739 Bauer, H., Claeys, M., Vermeylen, R., Schueller, E., Weinke, G., Berger, A., and Puxbaum,
740 H.: Arabitol and mannitol as tracers for the quantification of airborne fungal spores,
741 Atmos. Environ., 42, 588–593, 2008.
742 Bikkina, S., Haque, M. M., Sarin, M., and Kawamura, K.: Tracing the relative significance of
743 primary versus secondary organic aerosols from biomass burning plumes over coastal
744 ocean using sugar compounds and stable carbon isotopes, ACS Earth Space Chem., 3,
745 1471-1484, https://doi.org/10.1021/acsearthspacechem.9b00140, 2019.
746 Bikkina, S., Kawamura, K., Sakamoto, Y., and Hirokawa, J: Low molecular weight
747 dicarboxylic acids, oxocarboxylic acids and α-dicarbonyls as ozonolysis products of
748 isoprene: Implication for the gaseous-phase formation of secondary organic aerosols, Sci.
749 Total Environ., 769, 144472, https://doi.org/10.1016/j.scitotenv.2020.144472, 2021.
750 Brahney, J., Ballantyne, A. P., Sievers, C., and Neff, J. C.: Increasing Ca^{2+} deposition in the
751 western US: The role of mineral aerosols, Aeolian Res., 10, 77–87, 2013.
752 Birch, M. E., and Cary, R. A.: Elemental carbon-based method for monitoring occupational
753 exposures to particulate diesel exhaust, Aerosol Sci. Technol., 25 (3), 221−241, 1996.
754 Boreddy, S. K. R., Haque, M. M., and Kawamura, K.: Long term (2001–2012) trends of
755 carbonaceous aerosols from a remote island in the western North Pacific: an outflow
756 region of Asian pollutants, Atmos. Chem. Phys., 18, 1291–1306,
757 https://doi.org/10.5194/acp-18-1291-2018, 2018.
758 Broadgate, W. J., Liss, P. S., and Penkett, S. A.: Seasonal emissions of isoprene and other
759 reactive hydrocarbon gases from the ocean, Geophys. Res. Lett., 24, 2675-2678,
760 https://doi.org/10.1029/97GL02736, 1997.
761 Cheng, Y., Engling, G., He, K.-B., Duan, F.-K., Ma, Y.-L., Du, Z.-Y., Liu, J.-M., Zheng, M.,
762 and Weber, R. J.: Biomass burning contribution to Beijing aerosol, Atmos. Chem. Phys.,
763 13, 7765–7781, 2013.
764 Claeys, M., Graham, B., Vas, G., Wang, W., Vermeylen, R., Pashynska, V., Cafmeyer, J.,
765 Guyon, P., Andreae, M. O., Artaxo, P., and Maenhaut, W.: Formation of secondary
766 organic aerosols through photooxidation of isoprene, Science, 303(5661), 1173–1176,
767 2004.
768 Claeys, M., Szmigielski, R., Kourtchev, I., van der Veken, P., Vermeylen, R., Maenhaut, W.,
769 Jaoui, M., Kleindienst, T. E., Lewandowski, M., Offenberg, J., and Edney, E. O.:
770 Hydroxydicarboxylic acids: Markers for secondary organic aerosol from the
771 photooxidation of α-pinene, Environ. Sci. Technol., 41(5), 1628–1634, 2007.
772 Conte, L., Szopa, S., Aumont, O., Gros, V., and Bopp, L.: Sources and sinks of isoprene in
773 the global open ocean: Simulated patterns and emissions to the atmosphere, J. Geophys.
774 Res. Ocean., 9, e2019JC015946, https://doi.org/10.1029/2019JC015946, 2020.
775 Deguillaume, L., Leriche, M., Amato, P., Ariya, P. A., Delort, A.-M., Pöschl, U.,
776 Chaumerliac, N., Bauer, H., Flossmann, A. I., and Morris, C. E.: Microbiology and
777 atmospheric processes: chemical interactions of primary biological aerosols,
778 Biogeosciences, 5, 1073–1084, 2008.
779 Ding, X., Wang, X. M., Gao, B., Fu, X. X., He, Q. F., Zhao, X. Y., Yu, J. Z., and Zheng, M.:
780 Tracer-based estimation of secondary organic carbon in the Pearl River Delta, south
781 China, J. Geophys. Res. Atmos., 117, D05313, https://doi.org/10.1029/2011JD016596,
782 2012.

783 Ding, X., He, Q. F., Shen, R. Q., Yu, Q. Q., and Wang, X. M.: Spatial distributions of
784 secondary organic aerosols from isoprene, monoterpenes, β-caryophyllene, and aromatics
785 over China during summer, J. Geophys. Res., 119, 11877-11891,
786 https://doi.org/10.1002/2014JD021748, 2014.
787 Engling, G., Carrico, C. M., Kreldenweis, S. M., Collett, J. L., Day, D. E., Malm, W. C.,
788 Lincoln, E., Hao, W. M., Iinuma, Y., and Herrmann, H.: Determination of levoglucosan
789 in biomass combustion aerosol by high-performance anion-exchange chromatography
790 with pulsed amperometric detection, Atmos. Environ., 40, S299–S311, 2006.
791 Engling, G., Lee, J. J., Tsai, Y. W., Lung, S. C. C., Chou, C. C. K., and Chan, C. Y.: Size-
792 resolved anhydrosugar composition in smoke aerosol from controlled field burning of rice
793 straw, Aerosol Sci. Technol., 43(7), 662–672,
794 https://doi.org/10.1080/02786820902825113, 2009.
795 Fabbri, D., Marynowski, L., Fabianska, M. J., Zaton, M., and Simoneit, B. R. T.:
796 Levoglucosan and other cellulose markers in pyrolysates of miocene lignites:
797 Geochemical and environmental implications, Environ. Sci. Technol., 42(8), 2957–2963,
798 https://doi.org/10.1021/Es7021472, 2008.
799 Fine, P. M., Cass, G. R., and Simoneit, B. R. T.: Chemical characterization of fine particle
800 emissions from fireplace combustion of woods grown in the northeastern United States,
801 Environ. Sci. Technol., 35(13), 2665–2675, 2001.
802 Fine, P. M., Cass, G. R., and Simoneit, B. R. T.: Chemical characterization of fine particle
803 emissions from the fireplace combustion of wood types grown in the Midwestern and
804 Western United States, Environ. Eng. Sci., 21(3), 387–409, 2004.
805 Fraser, M. P. and Lakshmanan, K.: Using levoglucosan as a molecular marker for the long-
806 range transport of biomass combustion aerosols, Environ. Sci. Technol., 34(21), 4560–
807 4564, https://doi.org/10.1021/es991229l, 2000.
808 Fu, P., Kawamura, K., Kanaya, Y., and Wang, Z.: Contributions of biogenic volatile organic
809 compounds to the formation of secondary organic aerosols over Mt. Tai, Central East
810 China, Atmos. Environ., 44, 4817-4826, https://doi.org/10.1016/j.atmosenv.2010.08.040,
811 2010a.
812 Fu, P., Kawamura, K., Kobayashi, M., and Simoneit, B. R. T.: Seasonal variations of sugars
813 in atmospheric particulate matter from Gosan, Jeju Island: Significant contributions of
814 airborne pollen and Asian dust in spring, Atmos. Environ., 55, 234–239,
815 https://doi.org/10.1016/j.atmosenv.2012.02.061, 2012a.
816 Fu, P. Q., Kawamura, K., Okuzawa, K., Aggarwal, S. G., Wang, G., Kanaya, Y., and Wang,
817 Z.: Organic molecular compositions and temporal variations of summertime mountain
818 aerosols over Mt. Tai, North China Plain, J. Geophys. Res. Atmos., 113, D1910,
819 https://doi.org/10.1029/2008JD009900, 2008.
820 Fu, P. Q., Kawamura, K., and Barrie, L. A.: Photochemical and other sources of organic
821 compounds in the Canadian high Arctic aerosol pollution during winter-spring, Environ.
822 Sci. Technol., 43(2), 286–292, 2009a.
823 Fu, P. Q., Kawamura, K., Chen, J., and Barrie, L. A.: Isoprene, monoterpene, and
824 sesquiterpene oxidation products in the high Arctic aerosols during late winter to early
825 summer, Environ. Sci. Technol., 43(11), 4022–4028, 2009b.

826 Fu, P. Q., Kawamura, K., Pavuluri, C. M., Swaminathan, T., and Chen, J.: Molecular
827 characterization of urban organic aerosol in tropical India: contributions of primary
828 emissions and secondary photooxidation, Atmos. Chem. Phys., 10(6), 2663–2689, 2010b.
829 Fu, P. Q., Kawamura, K., and Miura, K.: Molecular characterization of marine organic
830 aerosols collected during a round-the-world cruise, J. Geophys. Res., 116, D13302,
831 https://doi.org/10.1029/2011jd015604, 2011.
832 Fu, P. Q., Kawamura, K., Chen, J., Li, J., Sun, Y. L., Liu, Y., Tachibana, E., Aggarwal, S. G.,
833 Okuzawa, K., Tanimoto, H., Kanaya, Y., and Wang, Z. F.: Diurnal variations of organic
834 molecular tracers and stable carbon isotopic composition in atmospheric aerosols over
835 Mt. Tai in the North China Plain: an influence of biomass burning, Atmos. Chem. Phys.,
836 12(18), 8359–8375, https://doi.org/10.5194/Acp-12-8359-2012, 2012b.
837 Gómez-González, Y., Wang, W., Vermeylen, R., Chi, X., Neirynck, J., Janssens, I. A.,
838 Maenhaut, W., and Claeys, M.: Chemical characterisation of atmospheric aerosols during
839 a 2007 summer field campaign at Brasschaat, Belgium: Sources and source processes of
840 biogenic secondary organic aerosol, Atmos. Chem. Phys., 12, 125-138,
841 https://doi.org/10.5194/acp-12-125-2012, 2012.
842 Graham, B., Guyon, P., Taylor, P. E., Artaxo, P., Maenhaut, W., Glovsky, M. M., Flagan, R.
843 C., and Andreae, M. O.: Organic compounds present in the natural Amazonian aerosol:
844 Characterization by gas chromatography-mass spectrometry, J. Geophys. Res. Atmos.,
845 108, D24, 4766, https://doi.org/10.1029/2003JD003990, 2003.
846 Griffin, R. J., Cocker, D. R., Seinfeld, J. H., and Dabdub, D.: Estimate of global atmospheric
847 organic aerosol from oxidation of biogenic hydrocarbons, Geophys. Res. Lett., 26, 2721–
848 2724, 1999.
849 Guenther, A., Hewitt, C. N., Erickson, D., Fall, R., Geron, C., Graedel, T., Harley, P.,
850 Klinger, L., Lerdau, M., McKay, W. A., Pierce, T., Scholes, B. R. S., Tallamraju, R.,
851 Taylor, J., and Zimmerman, P.: A global model of natural volatile organic compound
852 emissions, J. Geophys. Res., 100(D5), 8873–8892, 1995.
853 Guenther, A., Karl, T., Harley, P., Wiedinmyer, C., Palmer, P. I., and Geron, C.: Estimates of
854 global terrestrial isoprene emissions using MEGAN (Model of Emissions of Gases and
855 Aerosols from Nature), Atmos. Chem. Phys., 6, 3181–3210, 2006.
856 Haque, M. M., Kawamura, K., Deshmukh, D. K., Fang, C., Song, W., Mengying, B., and
857 Zhang, Y. L.: Characterization of organic aerosols from a Chinese megacity during
858 winter: Predominance of fossil fuel combustion, Atmos. Chem. Phys., 19, 5147-5164,
859 https://doi.org/10.5194/acp-19-5147-2019, 2019.
860 Heald, C. L. and Spracklen, D. V.: Atmospheric budget of primary biological aerosol
861 particles from fungal spores, Geophys. Res. Lett., 36, L09806,
862 https://doi.org/10.1029/2009GL037493, 2009.
863 Heald, C. L., Henze, D. K., Horowitz, L. W., Feddema, J., Lamarque, J. F., Guenther, A.,
864 Hess, P. G., Vitt, F., Seinfeld, J. H., Goldstein, A. H., and Fung, I.: Predicted change in
865 global secondary organic aerosol concentrations in response to future climate, emissions,
866 and land use change, J. Geophys. Res., 113(D5), https://doi.org/10.1029/2007jd009092,
867 2008.

Hennigan, C. J., Sullivan, A. P., Collett, J. L., and Robinson, A. L.: Levoglucosan stability in biomass burning particles exposed to hydroxyl radicals, Geophys. Res. Lett., 37, https://doi.org/10.1029/2010GL043088, 2010.

Hu, Q. H., Xie, Z. Q., Wang, X. M., Kang, H., He, Q. F., and Zhang, P.: Secondary organic aerosols over oceans via oxidation of isoprene and monoterpenes from Arctic to Antarctic, Sci. Rep., 3, 3119, https://doi.org/10.1038/srep02280, 2013.

Huang, R. J., Zhang, Y-L., Bozzetti, C., Ho, K-F., Cao, J-J., Han, Y., Daellenbach, K. R., Slowik, J. G., Platt, S. M., Canonaco, F., Zotter, P., Wolf, R., Pieber, S. M., Bruns, E. A., Crippa, M., Ciarelli, G., Piazzalunga, A., Schwikowski, M., Abbaszade, G., Schnelle-Kreis, J., Zimmermann, R., An, Z., Szidat, S., Baltensperger, U., Haddad, I. E., and Préôt, A. S. H.: High secondary aerosol contribution to particulate pollution during haze events in China, Nature, 514, 218–222, https://doi.org/10.1038/nature13774, 2014.

Huebert, B. J., Bates, T., Russell, P. B., Shi, G. Y., Kim, Y. J., Kawamura, K., Carmichael, G., and Nakajima, T.: An overview of ACE-Asia: Strategies for quantifying the relationships between Asian aerosols and their climatic impacts, J. Geophys. Res. Atmos., 108(D23), 8633, https://doi.org/10.1029/2003JD003550, 2003.

Jia, Y. L. and Fraser, M.: Characterization of saccharides in size-fractionated ambient particulate matter and aerosol sources: The contribution of primary biological aerosol particles (PBAPs) and soil to ambient particulate matter, Environ. Sci. Technol., 45(3), 930–936, https://doi.org/10.1021/es103104e, 2011.

Kanakidou, M., Seinfeld, J. H., Pandis, S. N., Barnes, I., Dentener, F. J., Facchini, M. C., Van Dingenen, R., Ervens, B., Nenes, A., Nielsen, C. J., Swietlicki, E., Putaud, J. P., Balkanski, Y., Fuzzi, S., Horth, J., Moortgat, G. K., Winterhalter, R., Myhre, C. E. L., Tsigaridis, K., Vignati, E., Stephanou, E. G., and Wilson, J.: Organic aerosol and global climate modelling: a review, Atmos. Chem. Phys., 5, 1053–1123, 2005.

Kang, M., Ren, L., Ren, H., Zhao, Y., Kawamura, K., Zhang, H., Wei, L., Sun, Y., Wang, Z., and Fu, P.: Primary biogenic and anthropogenic sources of organic aerosols in Beijing, China: Insights from saccharides and n-alkanes, Environ. Pollut., 243, 1579-1587, https://doi.org/10.1016/j.envpol.2018.09.118, 2018a.

Kang, M., Fu, P., Kawamura, K., Yang, F., Zhang, H., Zang, Z., Ren, H., Ren, L., Zhao, Y., Sun, Y., and Wang, Z.: Characterization of biogenic primary and secondary organic aerosols in the marine atmosphere over the East China Sea, Atmos. Chem. Phys., 19, 13947-13967, https://doi.org/10.5194/acp-18-13947-2018, 2018b.

Kawamura, K., Kobayashi, M., Tsubonuma, N., Mochida, M., Watanabe, T., and Lee, M.: Organic and inorganic compositions of marine aerosols from East Asia: Seasonal variations of water-soluble dicarboxylic acids, major ions, total carbon and nitrogen, and stable C and N isotopic composition, in geochemical investigations in earth and space science: A Tribute to Isaac R. Kaplan, edited by R. J. Hill, J. Leventhal, Z. Aizenshtat, M. J. Baedecker, G. Claypool, R. Eganhouse, M. Goldhaber, and K. Peters, pp. 243–265, The Geochemical Society, 2004.

Kessler, S. H., Smith, J. D., Che, D. L., Worsnop, D. R., Wilson, K. R., and Kroll, J. H.: Chemical sinks of organic aerosol: Kinetics and products of the heterogeneous oxidation of erythritol and levoglucosan, Environ. Sci. Technol., 44(18), 7005–7010, https://doi.org/10.1021/Es101465m, 2010.

912 Kleindienst, T. E., Jaoui, M., Lewandowski, M., Offenberg, J. H., Lewis, C. W., Bhave, P.
913 V., and Edney, E. O.: Estimates of the contributions of biogenic and anthropogenic
914 hydrocarbons to secondary organic aerosol at a southeastern US location, Atmos.
915 Environ., 41, 8288–8300, 2007.
916 Kourtchev, I., Hellebust, S., Bell, J. M., O'Connor, I. P., Healy, R. M., Allanic, A., Healy, D.,
917 Wenger, J. C., and Sodeau, J. R.: The use of polar organic compounds to estimate the
918 contribution of domestic solid fuel combustion and biogenic sources to ambient levels of
919 organic carbon and $PM_{2.5}$ in Cork Harbour, Ireland, Sci. Total Environ., 11, 2143-2155,
920 https://doi.org/10.1016/j.scitotenv.2011.02.027, 2011.
921 Kroll, J. H., Ng, N. L., Murphy, S. M., Flagan, R. C., and Seinfeld, J. H.: Secondary organic
922 aerosol formation from isoprene photooxidation under high-NOx conditions, Geophys.
923 Res. Lett., 32(18), L18808, https://doi.org/10.1029/2005gl023637, 2005.
924 Kroll, J. H., Ng, N. L., Murphy, S. M., Flagan, R. C., and Seinfeld, J. H.: Secondary organic
925 aerosol formation from isoprene photooxidation, Environ. Sci. Technol., 40, 1869–1877,
926 2006.
927 Kundu, S., Kawamura, K., and Lee, M.: Seasonal variations of diacids, ketoacids, and α-
928 dicarbonyls in aerosols at Gosan, Jeju Island, South Korea: Implications for sources,
929 formation, and degradation during long-range transport, J. Geophys. Res., 115, D19307,
930 https://doi.org/10.1029/2010jd013973, 2010.
931 Lewis, D. H. and Smith, D. C.: Sugar alcohols (polyols) in fungi and green plants: 1.
932 Distributions, physiology and metabolism, New Phytol., 66, 143–184, 1967.
933 Liu, J., Chu, B., Chen, T., Liu, C., Wang, L., Bao, X., and He, H.: Secondary organic aerosol
934 formation from ambient air at an urban site in Beijing: Effects of OH exposure and
935 precursor concentrations, Environ. Sci. Technol., 52, 6834-6841,
936 https://doi.org/10.1021/acs.est.7b05701, 2018.
937 Medeiros, P. M. and Simoneit, B. R. T.: Analysis of sugars in environmental samples by gas
938 chromatography-mass spectrometry, J. Chromatogr. A, 1141(2), 271–278,
939 https://doi.org/10.1016/j.chroma.2006.12.017, 2007.
940 Medeiros, P. M., Conte, M. H., Weber, J. C., and Simoneit, B. R. T.: Sugars as source
941 indicators of biogenic organic carbon in aerosols collected above the Howland
942 Experimental Forest, Maine, Atmos. Environ., 40(9), 1694–1705, 2006.
943 Mohn, J., Szidat, S., Fellner, J., Rechberger, H., Quartier, R., Buchmann, B., and
944 Emmenegger, L.: Determination of biogenic and fossil CO_2 emitted by waste incineration
945 based on $^{14}CO_2$ and mass balances, Bioresour. Technol., 99, 6471-6479,
946 https://doi.org/10.1016/j.biortech.2007.11.042, 2008.
947 Müller, L., Reinnig, M. C., Naumann, K. H., Saathoff, H., Mentel, T. F., Donahue, N. M.,
948 and Hoffmann, T.: Formation of 3-methyl-1,2,3-butanetricarboxylic acid via gas phase
949 oxidation of pinonic acid - A mass spectrometric study of SOA aging, Atmos. Chem.
950 Phys., 12, 1483-1496, https://doi.org/10.5194/acp-12-1483-2012, 2012.
951 Nakajima, T., Yoon, S. C., Ramanathan, V., Shi, G. Y., Takemura, T., Higurashi, A.,
952 Takamura, T., Aoki, K., Sohn, B. J., Kim, S. W., Tsuruta, H., Sugimoto, N., Shimizu, A.,
953 Tanimoto, H., Sawa, Y., Lin, N. H., Lee, C. T., Goto, D., and Schutgens, N.: Overview of
954 the atmospheric brown cloud east Asian regional experiment 2005 and a study of the

aerosol direct radiative forcing in east Asia, J. Geophys. Res. Atmos., 112, D24S91, https://doi.org/10.1029/2007JD009009, 2007.

Ng, N. L., Kwan, A. J., Surratt, J. D., Chan, A. W. H., Chhabra, P. S., Sorooshian, A., Pye, H. O. T., Crounse, J. D., Wennberg, P. O., Flagan, R. C., and Seinfeld, J. H.: Secondary organic aerosol (SOA) formation from reaction of isoprene with nitrate radicals (NO_3), Atmos. Chem. Phys., 8(14), 4117–4140, 2008.

Offenberg, J., Lewis, C., Lewandowski, M., Jaoui, M., Kleindienst, T. E., and Edney, E. O.: Contributions of toluene and α-pinene to SOA formed in an irradiated toluene/r-pinene/NOx/air mixture: Comparison of results using ^{14}C content and SOA organic tracer methods, Environ. Sci. Technol., 41, 3972–3976, 2007.

Pashynska, V., Vermeylen, R., Vas, G., Maenhaut, W., and Claeys, M.: Development of a gas chromatographic/ion trap mass spectrometric method for the determination of levoglucosan and saccharidic compounds in atmospheric aerosols. Application to urban aerosols, J. Mass Spectrom., 37(12), 1249–1257, 2002.

Pio, C., Legrand, M., Alves, C. A., Oliveira, T., Afonso, J., Caseiro, A., Puxbaum, H., Sánchez-Ochoa, A., and Gelencsér, A.: Chemical composition of atmospheric aerosols during the 2003 summer intense forest fire period, Atmos. Environ., 42, 7530–7543, 2008.

Ramanathan, V., Li, F., Ramana, M. V., Praveen, P. S., Kim, D., Corrigan, C. E., Nguyen, H., Stone, E. A., Schauer, J. J., Carmichael, G. R., Adhikary, B., and Yoon, S. C.: Atmospheric brown clouds: Hemispherical and regional variations in long-range transport, absorption, and radiative forcing, J. Geophys. Res. Atmos., 112, D22S21, https://doi.org/10.1029/2006JD008124, 2007.

Robinson, A. L., Donahue, N. M., Shrivastava, M. K., Weitkamp, E. A., Sage, A. M., Grieshop, A. P., Lane, T. E., Pierce, J. R., and Pandis, S. N.: Rethinking organic aerosols: Semivolatile emissions and photochemical aging, Science, 315, 1259–1262, 2007.

Salazar, G., Zhang, Y. L., Agrios, K., and Szidat, S.: Development of a method for fast and automatic radiocarbon measurement of aerosol samples by online coupling of an elemental analyzer with a MICADAS AMS, Nucl. Instruments Methods Phys. Res. Sect. B Beam Interact. with Mater. Atoms, 361, 163-167, https://doi.org/10.1016/j.nimb.2015.03.051, 2015.

Schmidl, C., Marr, I. L., Caseiro, A., Kotianova, P., Berner, A., Bauer, H., Kasper-Giebl, A., and Puxbaum, H.: Chemical characterisation of fine particle emissions from wood stove combustion of common woods growing in mid-European Alpine regions, Atmos. Environ., 42, 126–141, 2008a.

Schmidl, C., Bauer, H., Dattler, A., Hitzenberger, R., Weissenboeck, G., Marr, I. L., and Puxbaum, H.: Chemical characterisation of particle emissions from burning leaves, Atmos. Environ., 42(40), 9070–9079, https://doi.org/10.1016/J.Atmosenv.2008.09.010, 2008b.

Shaw, S. L., Gantt, B., and Meskhidze, N.: Production and emissions of marine isoprene and monoterpenes: A Review, Adv. Meteorol., 2010, 408696, https://doi.org/10.1155/2010/408696, 2010.

Sheesley, R. J., Schauer, J. J., Chowdhury, Z., Cass, G. R., and Simoneit, B. R. T.: Characterization of organic aerosols emitted from the combustion of biomass indigenous

999 to South Asia, J. Geophys. Res., 108 (D9), 4285, https://doi.org/10.1029/2002JD002981,
1000 2003.
1001 Simoneit, B. R. T.: Biomass burning-a review of organic tracers for smoke from incomplete
1002 combustion, Appl. Geochem., 17, 129–162, 2002.
1003 Simoneit, B. R. T., Schauer, J. J., Nolte, C. G., Oros, D. R., Elias, V. O., Fraser, M. P.,
1004 Rogge, W. F., and Cass, G. R.: Levoglucosan, a tracer for cellulose in biomass burning
1005 and atmospheric particles, Atmos. Environ., 33(2), 173–182,
1006 https://doi.org/10.1016/S1352-2310(98)00145-9, 1999.
1007 Simoneit, B. R. T., Elias, V. O., Kobayashi, M., Kawamura, K., Rushdi, A. I., Medeiros, P.
1008 M., Rogge, W. F., and Didyk, B. M.: Sugars-dominant water-soluble organic compounds
1009 in soils and characterization as tracers in atmospheric particulate matter, Environ. Sci.
1010 Technol., 38(22), 5939–5949, 2004a.
1011 Simoneit, B. R. T., Kobayashi, M., Mochida, M., Kawamura, K., Lee, M., Lim, H-J., Turpin,
1012 B. J., and Komazaki, Y.: Composition and major sources of organic compounds of
1013 aerosol particulate matter sampled during the ACE-Asia campaign, J. Geophys. Res.,
1014 109(D19), D19S10, https://doi.org/10.1029/2004jd004598, 2004b.
1015 Singh, N., Mhawish, A., Deboudt, K., Singh, R. S., and Banerjee, T.: Organic aerosols over
1016 Indo-Gangetic Plain: Sources, distributions and climatic implications, Atmos. Environ.,
1017 157, 59-74, https://doi.org/10.1016/j.atmosenv.2017.03.008, 2017.
1018 Stein, A. F., Draxler, R. R., Rolph, G. D., Stunder, B. J. B., Cohen, M. D., and Ngan, F.:
1019 Noaa's hysplit atmospheric transport and dispersion modeling system, Bull. Am.
1020 Meteorol. Soc., 96, 2059-2077, https://doi.org/10.1175/BAMS-D-14-00110.1, 2015.
1021 Stuiver, M. and Polach, H. A.: Discussion: Reporting of ^{14}C data, Radiocarbon, 19(3),
1022 355−363, 1997.
1023 Sullivan, A. P., Holden, A. S., Patterson, L. A., McMeeking, G. R., Kreidenweis, S. M.,
1024 Malm, W. C., Hao, W. M., Wold, C. E., and Collett, Jr., J. L.: A method for smoke
1025 marker measurements and its potential application for determining the contribution of
1026 biomass burning from wildfires and prescribed fires to ambient $PM_{2.5}$ organic carbon, J.
1027 Geophys. Res., 113, D22302, https://doi.org/10.1029/2008JD010216, 2008.
1028 Surratt, J. D., Murphy, S. M., Kroll, J. H., Ng, N. L., Hildebrandt, L., Sorooshian, A.,
1029 Szmigielski, R., Vermeylen, R., Maenhaut, W., Claeys, M., Flagan, R. C., and Seinfeld, J.
1030 H.: Chemical composition of secondary organic aerosol formed from the photooxidation
1031 of isoprene, J. Phys. Chem. A, 110(31), 9665–9690, 2006.
1032 Surratt, J. D., Chan, A. W. H., Eddingsaas, N. C., Chan, M. N., Loza, C. L., Kwan, A. J.,
1033 Hersey, S. P., Flagan, R. C., Wennberg, P. O., and Seinfeld, J. H.: Reactive intermediates
1034 revealed in secondary organic aerosol formation from isoprene, Proc. Natl. Acad. Sci.
1035 USA, 107(15), 6640–6645, 2010.
1036 Szidat, S., Jenk, T. M., Synal, H. A., Kalberer, M., Wacker, L., Hajdas, I., Kasper-Giebl, A.,
1037 and Baltensperger, U.: Contributions of fossil fuel, biomass-burning, and biogenic
1038 emissions to carbonaceous aerosols in Zurich as traced by ^{14}C, J. Geophys. Res. Atmos.,
1039 111, D07206, https://doi.org/10.1029/2005JD006590, 2006.
1040 Szmigielski, R., Surratt, J. D., Gómez-González, G., Van der Veken, P., Kourtchev, I.,
1041 Vermeylen, R., Blockhuys, F., Jaoui, M., Kleindienst, T. E., Lewandowski, M.,
1042 Offenberg, J. H., Edney, E. O., Seinfeld, J. H., Maenhaut, W., and Claeys, M.: 3-Methyl-

1,2,3-butanetricarboxylic acid: An atmospheric tracer for terpene secondary organic aerosol, Geophys. Res. Lett., 34, L24811, https://doi.org/10.1029/2007GL031338, 2007.

Theodosi, C., Panagiotopoulos, C., Nouara, A., Zarmpas, P., Nicolaou, P., Violaki, K., Kanakidou, M., Sempéré, R., and Mihalopoulos, N.: Sugars in atmospheric aerosols over the Eastern Mediterranean, Prog. Oceanogr., 163, Special Issue: SI, 70-81, https://doi.org/10.1016/j.pocean.2017.09.001, 2018.

Tyagi, P., Kawamura, K., Kariya, T., Bikkina, S., Fu, P., and Lee, M.: Tracing atmospheric transport of soil microorganisms and higher plant waxes in the East Asian outflow to the North Pacific Rim by using hydroxy fatty acids: Year-round observations at Gosan, Jeju Island, J. Geophys. Res., 122, 4112-4131, https://doi.org/10.1002/2016JD025496, 2017.

Verma, S. K., Kawamura, K., Chen, J., Fu, P., and Zhu, C.: Thirteen years of observations on biomass burning organic tracers over Chichijima Island in the western North Pacific: An outflow region of Asian aerosols, J. Geophys. Res., 120, 4155-4168, https://doi.org/10.1002/2014JD022224, 2015.

Verma, S. K., Kawamura, K., Chen, J., and Fu, P.: Thirteen years of observations on primary sugars and sugar alcohols over remote Chichijima Island in the western North Pacific, Atmos. Chem. Phys., 18, 81-101, https://doi.org/10.5194/acp-18-81-2018, 2018.

Wang, G. and Kawamura, K.: Molecular characteristics of urban organic aerosols from Nanjing: A case study of a mega-city in China, Environ. Sci. Technol., 39(19), 7430–7438, 2005.

Wang, G. H., Kawamura, K., and Lee, M.: Comparison of organic compositions in dust storm and normal aerosol samples collected at Gosan, Jeju Island, during spring 2005, Atmos. Environ., 43(2), 219–227, https://doi.org/10.1016/J.Atmosenv.2008.09.046, 2009a.

Wang, G. H., Li, J. J., Cheng, C. L., Zhou, B. H., Xie, M. J., Hu, S. Y., Meng, J. J., Sun, T., Ren, Y. Q., Cao, J. J., Liu, S. X., Zhang, T., and Zhao, Z. Z.: Observation of atmospheric aerosols at Mt. Hua and Mt. Tai in central and east China during spring 2009-Part 2: Impact of dust storm on organic aerosol composition and size distribution, Atmos. Chem. Phys., 12(9), 4065–4080, 2012.

Wang, W., Kourtchev, I., Graham, B., Cafmeyer, J., Maenhaut, W., and Claeys, M.: Characterization of oxygenated derivatives of isoprene related to 2-methyltetrols in Amazonian aerosols using trimethylsilylation and gas chromatography/ion trap mass spectrometry, Rapid Commun. Mass Spectrom., 19, 1343–1351, 2005.

Wang, Y. Q., Zhang, X. Y., and Draxler, R. R.: TrajStat: GIS-based software that uses various trajectory statistical analysis methods to identify potential sources from long-term air pollution measurement data, Environ. Model. Softw., 24, 938-939, https://doi.org/10.1016/j.envsoft.2009.01.004, 2009b.

Wu, J., Kong, S., Zeng, X., Cheng, Y., Yan, Q., Zheng, H., Yan, Y., Zheng, S., Liu, D., Zhang, X., Fu, P., Wang, S., and Qi, S.: First high-resolution emission inventory of levoglucosan for biomass burning and non-biomass burning sources in China, Environ. Sci. Technol., 55, 3, 1497–1507, 2021.

Yan, C., Zheng, M., Sullivan, A. P., Shen, G., Chen, Y., Wang, S., Zhao, B., Cai, S., Desyaterik, Y., Li, X., Zhou, T., Gustafsson, Ö., and Collett, J. L.: Residential coal combustion as a source of levoglucosan in China, Environ. Sci. Technol., 52, 3, 1665–1674, https://doi.org/10.1021/acs.est.7b05858, 2018.

Yttri, K. E., Dye, C., and Kiss, G.: Ambient aerosol concentrations of sugars and sugar-alcohols at four different sites in Norway, Atmos. Chem. Phys., 7, 4267–4279, 2007.

Zangrando, R., Barbaro, E., Kirchgeorg, T., Vecchiato, M., Scalabrin, E., Radaelli, M., Đorđević, D., Barbante, C., and Gambaro, A.: Five primary sources of organic aerosols in the urban atmosphere of Belgrade (Serbia), Sci. Total Environ., 571, 1441-1453, https://doi.org/10.1016/j.scitotenv.2016.06.188, 2016.

Zhang, Y. L., Perron, N., Ciobanu, V. G., Zotter, P., Minguillón, M. C., Wacker, L., Prévôt, A. S. H., Baltensperger, U., and Szidat, S.: On the isolation of OC and EC and the optimal strategy of radiocarbon-based source apportionment of carbonaceous aerosols, Atmos. Chem. Phys., 12, 10841-10856, https://doi.org/10.5194/acp-12-10841-2012, 2012.

Zhang, Y. L., Huang, R. J., El Haddad, I., Ho, K. F., Cao, J. J., Han, Y., Zotter, P., Bozzetti, C., Daellenbach, K. R., Canonaco, F., Slowik, J. G., Salazar, G., Schwikowski, M., Schnelle-Kreis, J., Abbaszade, G., Zimmermann, R., Baltensperger, U., Prévôt, A. S. H., and Szidat, S.: Fossil vs. non-fossil sources of fine carbonaceous aerosols in four Chinese cities during the extreme winter haze episode of 2013, Atmos. Chem. Phys., 15(3), 1299-1312, https://doi.org/10.5194/acp-15-1299-2015, 2015.

Zhang, Y. L., Kawamura, K., Agrios, K., Lee, M., Salazar, G., and Szidat, S.: Fossil and nonfossil sources of organic and elemental carbon aerosols in the outflow from Northeast China, Environ. Sci. Technol., 50, 6284-6292, https://doi.org/10.1021/acs.est.6b00351, 2016.

Zhu, C., Kawamura, K., and Kunwar, B.: Effect of biomass burning over the western North Pacific Rim: wintertime maxima of anhydrosugars in ambient aerosols from Okinawa., Atmos. Chem. Phys., 15, 1959–1973, https://doi.org/10.5194/acp-15-1959-2015, 2015a.

Zhu, C., Kawamura, K., and Kunwar, B.: Organic tracers of primary biological aerosol particles at subtropical Okinawa island in the western North pacific rim, J. Geophys. Res., 120, 5504-5523, https://doi.org/10.1002/2015JD023611, 2015b.

1123 **Table 1.** Concentrations of identified sugar compounds and BSOA tracers (ng m^{-3}) in the atmospheric
1124 aerosol samples from Gosan.

Species	Annual	Summer	Fall	Winter	Spring
	Avg.[a] ± S.D.[b] Min.[c], Max.[d]	Avg. ± S.D. Min., Max.	Avg. ± S.D. Min., Max.	Avg. ± S.D. Min., Max.	Avg. ± S.D. Min., Max.
Anhydrosugars					
Levoglucosan (Lev)	17.6 ± 16.8 0.60, 45.9	2.92 ± 3.89 0.60, 9.81	21.7 ± 19.0 2.30, 43.9	39.2 ± 6.60 32.0, 45.9	12.7 ± 11.6 1.45, 33.4
Mannosan (Man)	1.57 ± 1.82 0.05, 6.74	0.18 ± 0.24 0.05, 0.61	1.69 ± 1.49 0.13, 3.66	3.63 ± 2.28 1.47, 6.74	1.31 ± 1.57 0.08, 4.08
Galactosan (Gal)	2.28 ± 2.10 0.14, 6.78	0.64 ± 0.68 0.14, 1.82	2.45 ± 2.13 0.35, 4.92	5.21 ± 1.64 3.40, 6.78	1.65 ± 1.26 0.50, 3.88
Primary Sugars					
Glucose	18.8 ± 27.1 2.45, 122	13.4 ± 18.2 2.45, 45.6	16.5 ± 15.7 2.68, 33.6	4.74 ± 3.14 2.88, 9.44	32.4 ± 41.1 4.87, 122
Fructose	10.3 ± 15.9 0.97, 74.0	4.90 ± 5.15 0.97, 13.7	7.48 ± 6.99 1.71, 16.2	3.82 ± 4.45 1.56, 10.5	19.8 ± 25.0 2.69, 74.0
Sucrose	16.1 ± 32.2 0.26, 140	1.46 ± 1.05 0.68, 3.28	9.74 ± 12.1 0.76, 27.2	8.87 ± 16.3 0.42, 33.3	35.1 ± 50.5 0.26, 140
Trehalose	2.42 ± 1.97 0.65, 7.03	2.72 ± 2.53 0.97, 6.98	3.71 ± 2.29 1.18, 7.03	1.21 ± 0.42 0.72, 1.63	1.98 ± 1.55 0.65, 5.33
Xylose	0.81 ± 0.65 0.04, 2.03	0.23 ± 0.23 0.04, 0.63	0.86 ± 0.68 0.14, 1.70	1.59 ± 0.37 1.21, 2.03	0.74 ± 0.55 0.16, 1.68
Sugar alcohols					
Arabitol	3.96 ± 4.24 0.47, 18.7	5.64 ± 7.46 1.20, 18.7	5.27 ± 3.51 2.27, 10.9	1.06 ± 0.60 0.47, 1.91	3.47 ± 2.19 1.18, 6.30
Mannitol	4.61 ± 5.54 0.25, 22.0	7.39 ± 8.65 1.71, 22.0	6.64 ± 6.03 1.69, 16.7	0.99 ± 0.45 0.55, 1.60	3.24 ± 2.67 0.25, 7.03
Erythritol	0.62 ± 0.43 0.12, 1.52	0.92 ± 0.53 0.42, 1.52	0.93 ± 0.33 0.55, 1.27	0.42 ± 0.27 0.16, 0.80	0.30 ± 0.12 0.12, 0.48
Inositol	0.34 ± 0.39 0.04, 1.53	0.29 ± 0.41 0.08, 1.03	0.56 ± 0.60 0.10, 1.53	0.13 ± 0.07 0.08, 0.23	0.35 ± 0.28 0.04, 0.73
Isoprene-SOA tracers					
2-MGA	0.99 ± 0.70 0.17, 2.79	1.61 ± 1.17 0.17, 2.79	0.95 ± 0.43 0.51, 1.61	0.67 ± 0.14 0.49, 0.81	0.76 ± 0.35 0.20, 1.32
Σ2-MLTs	1.04 ± 1.40 0.05, 5.81	2.48 ± 1.98 0.51, 5.81	1.34 ± 1.16 0.33, 2.74	0.20 ± 0.05 0.15, 0.26	0.29 ± 0.25 0.05, 0.82
ΣC5-alkene triols	0.20 ± 0.25 0.02, 1.17	0.46 ± 0.44 0.02, 1.17	0.13 ± 0.05 0.05, 0.18	0.09 ± 0.03 0.05, 0.13	0.14 ± 0.11 0.02, 0.30
Monoterpene-SOA tracers					
cis-pinonic acid	0.15 ± 0.14 0.02, 0.52	0.12 ± 0.13 0.03, 0.36	0.08 ± 0.06 0.02, 0.16	0.07 ± 0.03 0.02, 0.10	0.26 ± 0.17 0.08, 0.52
pinic acid	1.67 ± 1.01 0.72, 4.81	2.40 ± 1.67 0.99, 4.81	1.53 ± 0.57 0.75, 2.11	1.07 ± 0.25 0.84, 1.42	1.61 ± 0.78 0.72, 2.94
3-HGA	2.30 ± 2.38 0.19, 10.6	3.46 ± 4.39 0.19, 10.6	1.52 ± 0.77 0.76, 2.79	1.40 ± 0.39 0.94, 1.88	2.54 ± 1.83 0.38, 4.57
MBTCA	5.11 ± 4.54 0.29, 19.6	8.44 ± 6.88 3.00, 19.6	6.24 ± 3.64 1.17, 9.49	1.90 ± 0.85 0.97, 2.83	3.77 ± 2.96 0.29, 8.08

[a]Average, [b]Standard deviation, [c]Minimum, [d]Maximum. 2-MGA: 2-methylglyceric acid, 2-MLTs: 2-methyltetrols, 3-HGA: 3-hydroxyglutaric acid, MBTCA: 3-methyl-1,2,3-butanetricarboxylic acid.

1125

1126 **Table 2.** Statistical summary of diagnostic ratios and carbonaceous components contribution in Gosan
1127 aerosols.
1128

Species	Annual	Summer	Fall	Winter	Spring
	Avg.[a] ± S.D.[b] Min.[c], Max.[d]	Avg. ± S.D. Min., Max.	Avg. ± S.D. Min., Max.	Avg. ± S.D. Min., Max.	Avg. ± S.D. Min., Max.
Diagnostic ratios					
Lev/Man	15.1 ± 6.76 6.81, 31.3	17.1 ± 8.21 8.58, 28.4	13.7 ± 2.51 11.1, 17.3	13.5 ± 6.24 6.81, 21.7	15.4 ± 8.76 6.98, 31.3
Man/Gal	0.55 ± 0.32 0.10, 1.07	0.28 ± 0.13 0.10, 0.42	0.64 ± 0.20 0.37, 0.90	0.66 ± 0.27 0.43, 1.05	0.61 ± 0.43 0.16, 1.07
Lev/(Man + Gal)	4.27 ± 1.23 2.18, 6.56	3.12 ± 0.78 2.18, 4.03	5.08 ± 0.32 4.71, 5.51	4.85 ± 1.35 3.49, 6.56	4.17 ± 1.33 2.50, 6.45
Lev/$K^+ \times 10^{-2}$	5.73 ± 5.65 0.65, 23.2	1.00 ± 0.52 0.65, 1.91	3.94 ± 2.51 1.26, 6.30	12.3 ± 7.87 6.42, 23.2	6.65 ± 4.48 1.77, 15.3
Lev/OC × 10^{-2}	0.73 ± 0.66 0.08, 2.29	0.14 ± 0.10 0.08, 0.31	0.84 ± 0.61 0.12, 1.56	1.60 ± 0.67 0.99, 2.29	0.56 ± 0.40 0.11, 1.05
Lev/WSOC × 10^{-2}	1.09 ± 0.97 0.10, 3.46	0.20 ± 0.13 0.10, 0.42	1.25 ± 0.94 0.23, 2.21	2.33 ± 0.90 1.48, 3.46	0.92 ± 0.65 0.13, 1.69
2-MGA/2-MLTs	2.18 ± 1.59 0.33, 5.40	0.67 ± 0.43 0.33, 1.33	1.04 ± 0.49 0.41, 1.55	3.60 ± 1.43 1.90, 5.40	3.27 ± 1.17 1.60, 4.75
[e]P/MBTCA	0.62 ± 0.61 0.17, 5.90	3.22 ± 0.62 2.47, 3.89	3.62 ± 1.67 1.52, 5.90	1.68 ± 0.64 0.83, 2.38	1.73 ± 1.07 0.34, 3.32
Carbonaceous components					
Isoprene derived SOC (μgC m^{-3})	23.7 ± 23.9 2.26, 97.4	51.0 ± 32.4 8.08, 97.4	25.9 ± 17.9 8.54, 45.7	8.52 ± 1.07 7.46, 9.87	11.3 ± 6.80 2.26, 24.9
Isoprene SOC to OC (%)	1.45 ± 1.74 0.21, 6.40	3.56 ± 2.18 1.03, 6.40	1.46 ± 1.38 0.35, 3.48	0.35 ± 0.17 0.21, 0.57	0.57 ± 0.38 0.24, 1.35
Isoprene SOC to total SOC (%)	35.5 ± 15.5 13.5, 71.1	46.6 ± 20.3 26.0, 71.1	38.1 ± 10.4 21.1, 47.3	31.6 ± 7.05 24.0, 39.7	27.9 ± 15.5 13.5, 54.0
Monoterpene SOC (μgC m^{-3})	40.1 ± 33.3 7.18, 154	62.7 ± 56.5 19.2, 154	40.7 ± 20.0 11.8, 57.7	19.3 ± 5.61 14.0, 25.2	35.5 ± 23.5 7.18, 62.7
Monoterpene SOC to OC (%)	2.0 ± 1.47 0.37, 5.74	3.65 ± 1.58 2.44, 5.74	2.15 ± 1.45 0.48, 3.88	0.87 ± 0.58 0.37, 1.48	1.58 ± 0.84 0.54, 3.13
Monoterpene SOC to total SOC (%)	64.5 ± 15.5 28.9, 86.5	53.4 ± 20.3 28.9, 74.0	61.9 ± 10.4 52.7, 78.9	68.4 ± 7.05 60.3, 76.1	72.1 ± 15.5 46.0, 86.5

[e]P: *cis*-pinonic acid + pinic acid

Table 3. Comparisons of the mean concentration (ng m^{-3}) of anhydrosugars, sugar, and sugar alcohols in Gosan aerosols with those from different sites around the world.

Sampling sites	Sampling type	Sampling time	Anhydro-sugars	Primary sugars	Sugar alcohols	References
Gosan, South Korea	**TSP**	Summer Fall Winter Spring	**3.74** **25.9** **48.0** **15.7**	**22.8** **38.3** **20.2** **90.0**	**14.3** **13.4** **2.60** **7.36**	**This study**
Chennai, India	PM_{10}	Summer Winter	127 134	15.5 11.4	7.44 4.81	Fu et al., 2010b
Mt. Tai, China	TSP	Summer (June)	224	61.1	125	Fu et al., 2012b
Alert, Canada	TSP	Winter Spring	0.32 0.02	1.14 0.18	0.25 0.36	Fu et al., 2009a
Okinawa, western North Pacific	TSP	Summer Autumn Winter Spring	0.93 2.58 6.04 3.44	73.5 56.0 34.4 101	62.9 30.7 6.03 31.2	Zhu et al., 2015a, b
Chichijima, western North Pacific	TSP	Summer Autumn Winter Spring	0.32 0.85 2.40 0.94	32.8 22.0 14.2 24.2	38.6 35.1 3.93 15.5	Verma et al., 2015, 2018
Mt. Hua, China (Non-dust storm)	PM_{10}	April	57.8	92.5	22.4	Wang et al., 2012
Mt. Hua, China (Dust storm)	PM_{10}	April	44.5	162	25.7	Wang et al., 2012
Nanjing, China	$PM_{2.5}$	Summer Winter	151 (Lev) 268 (Lev)	59.3 42.3	11.8 13.4	Wang and Kawamura, 2005
Beijing, China	$PM_{2.5}$	Summer Autumn Winter Spring	14.5 129 254 81.4	6.63 17.2 41.5 33.9	3.31 13.7 17.8 12.3	Kang et al., 2018a
Belgrade, Serbia	TSP	Autumn	425 (Lev)	116	98.4	Zangrando et al., 2016
Maine, USA	PM_1	May-October	13.9	28	8.31	Medeiros et al., 2006
Crete, Greece	PM_{10}	Year-round	14.4	32.3	6.53	Theodosi et al., 2018